Haptic Rendering of Textures on Touch Surface Using Ultrasonic Actuation

by

Muhammad Khurram Saleem

A Dissertation Submitted to the
Graduate School of Sciences and Engineering
in Partial Fulfillment of the Requirements for
the Degree of

Doctor of Philosophy

in

Mechanical Engineering

KOÇ UNIVERSITY

February 15, 2019

Haptic Rendering of Textures on Touch Surface Using Ultrasonic Actuation

Koç University

Graduate School of Sciences and Engineering

This is to certify that I have examined this copy of a doctoral dissertation by

Muhammad Khurram Saleem

and have found that it is complete and satisfactory in all respects,
and that any and all revisions required by the final
examining committee have been made.

Committee Members:

Prof. Dr. Cagatay Basdogan (Thesis Advisor)

Assoc. Prof. Dr. Cetin Yilmaz

Assoc. Prof. Dr. Frederic Giraud

Assoc. Prof. Dr. Ipek Basdogan

Asst. Prof. Dr. Evren Samur

Date: 15th Feb, 2019

To my beloved family

ABSTRACT

To render tactile cues on a touchscreen by friction modulation, it is important to understand how human perceive a change in friction. This thesis aims to explore the tactile perception of changes in friction (called edges), and underlying perceptual mechanism. We first estimated the perceptual thresholds to detect a virtual edge, rendered by rising friction (RF) and falling friction (FF), while finger is sliding on the touch surface. Then, we conducted intensity scaling experiments and investigated the effect of finger sliding velocity, normal force, and rise/fall time of vibration amplitude (transition time) on the perceived intensity of a virtual edge. In order to better understand the role of contact mechanics, we also looked into the correlations between the perceived intensities of subjects and several parameters involved in contact. The results of our experiments showed that the contrast and rate of change in tangential force were best correlated with the perceived intensity. The subjects perceived RF more strongly than FF, particularly at higher tangential force contrast. The results also showed that transition time and normal force have significant effect on our tactile perception. In the second part, we investigated our ability to discriminate two consecutive edges, followed by discrimination and roughness perception of multiple edges (called periodic gratings). The results showed that discrimination of two consecutive edges was significantly influenced by edge sequence: FF followed by RF was discriminated more easily than the reverse order. On the other hand, periodic gratings generated by displaying consecutive edge sequence of FF followed by RF were perceived with the same acuity as compared to vice versa. We found that a relative difference of 14% in spatial period was required to discriminate two periodic gratings independent of the edge sequence. Moreover, the roughness perception of periodic gratings decreased with increasing spatial period for the range that we have inves-

tigated (spatial period > 2 mm), despite the lack of spatial cues on texture height. We also observed that rate of change in friction coefficient was better correlated with the roughness perception than the friction coefficient itself. These results will further help to understand and design of virtual textures for touch surfaces.

ÖZETÇE

Bir dokunmatik ekranda sürtünme değişimi ile dokunsal geri bildirim sağlamak için, insanın sürtünme değişimini nasıl algıladığını anlamak gereklidir. Bu tez, sürtünme ve arkasındaki fiziksel mekanizmaların dokunsal algımıza olan etkisini, ultrasonik bir frekansta titretilen bir cam ekran üzerinde, incelemeyi amaçlamaktadır. Bu amaçla, parmak ekran yüzeyinde kayarken, önce artan sürtünme (RF) ve sonra düşen sürtünme (FF) aracılığıyla oluşturulan sanal bir kenarı algılamak için gerekli algısal eşikleri ölçtük. Daha sonra, algısal yoğunluk ölçeklendirme deneyleri yaptık ve parmak kayma hızının, normal kuvvetin, ve titreşim genliğinin yükselme/düşme zamanının (geçiş zamanı) sanal bir kenarın algılanan yoğunluğu üzerindeki etkisini araştırdık. Bu algıda parmak temas mekaniğinin rolünü anlamak için, aynı zamanda deneklerin algılanan yoğunlukları ile temasa etkisi olan çeşitli parametreler arasındaki korelasyonları da inceledik. Deneylerimizin sonuçları, teğet kuvvetindeki kontrast ve değişim hızının algılanan yoğunluk ile korelasyonu olduğunu göstermiştir. Denekler, özellikle daha yüksek teğetsel kuvvet kontrastında, RF değerini FF 'den daha güçlü bir şekilde algıladı. Sonuçlar ayrıca geçiş süresinin ve normal kuvvetin dokunsal algımız üzerinde önemli bir etkisi olduğunu göstermiştir. çalışmamızın ikinci bölümünde, ardışık iki kenarı dokunsal algı vasıtasıyla ayırt etme yetimizi araştırdık, ardından çoklu kenarları (periyodik ızgaralar) dokunsal ayrıştırma becerimizi ve onların pürüzlülük algımıza etkisini inceledik. Sonuçlar, kenar diziliminin, ardışık iki kenarın ayrıştırılmasında önemli derecede etkili olduğunu göstermiştir: FF, ardından RF, ters sıradan daha kolay ayırt edildi. Öte yandan, önce FF ve sonra RF ardışık kenar dizisiyle oluşturulan periyodik ızgaralar, tam tersi ile aynı keskinlikte algılanmıştır. İki periyodik ızgarayı dokunsal yolla ayırt etmek için, konumsal bazda, % 14' lük göreceli bir farkın gerekli olduğunu bulduk. Ayrıca, periyodik sanal ızgaraların pürüzlülük algısı, artan ızgara

periyodu ile azalmıştır (not: periyodu 2 mm den daha büyük sanal ızgaralar incelendi). Ayrıca sürtünme katsayısındaki değişim hızının pürüzlülük algısı ile sürtünme katsayısından daha iyi bir korelasyon gösterdiği gözlemledi. Bu sonuçlar, mobil cihazlar, tüketici ürünleri, ve günümüz otomobillerinin içinde var olan dokunma yüzeyleri üzerinde, sanal işaretlerin ve dokuların kullanıcıya gösterimi ve tasarlanmasında yardımcı olacaktır.

ACKNOWLEDGMENTS

I would like to thank my advisor Dr. Cagatay Basdogan for his technical and moral support throughout my Ph.D. studies at Koc University.

I would like to thank Dr. Cetin Yilmaz for his valuable feedback in improving this work. I would like to thank Dr. Frederic Giraud and Dr. Evren Samur for their guidance in developing our ultrasonic tactile display.

I would like to thank all my lab fellows and friends who participated in our experiments with great enthusiasm and passion.

The Higher Edication Comission of Pakistan supported this work under Faculity Development Program UESTPs/UETs (Batch-III).

TABLE OF CONTENTS

LIST OF TABLES

LIST OF FIGURES

NOMENCLATURE

dF_t/dt Rate of change in tangential force

$d\mu/dt$ Rate of change in friction coefficient

Δt Duration between virtual edges

E_{seq} Edge sequence

FF Falling friction

$FF \rightarrow RF$ Falling edge followed by rising edge

F_n Normal force

F_t Tangential force

F_tC Tangential force contrast

f_v Finger velocity

GW Groove width

HFW High friction width

LFW Low friction width

R_{diff} Relative diference between spatial periods

RF Rising friction

$RF \to FF$ Rising edge followed by falling edge

R_{length} Rendering length

RW Ridge width

Δx Distance between virtual edges

S_n Normalized scores

SP Spatial period

t_r^{amp} Vibration amplitude transition time

t_r^{force} Force fransition time

μ Friction coefficient

μC Friction coefficient contrast

V_{amp} Vibrational amplitude

ω Temporal frequency

W_{frm} Waveform

Chapter 1

INTRODUCTION

Touch-enabled devices like smart-phones and tablets are ubiquitous now-a-days, and are being used everyday for telecommunication, e-commerce, games and entertainment, professional and social networking, information gathering on the Internet, etc. However, all the devices commercially available today provide visual and auditory feedback to their users but almost no tactile feedback, though it is known that tactile feedback improves task performance and realism when interacting with digital data. Moreover, tactile sensation is a significant factor for preference and admiration of certain consumer products due to their texture. Therefore, a great deal of research is being carried out in recent years to develop and study the techniques that can render tactile information on touch-enabled devices. In this regard, ultrasonic actuation and electrovibration are two emerging techniques that work on the principle of friction modulation. Ultrasonic actuation reduces, while the electrovibration increases the friction between fingerpad and touch surface. Two different mechanisms have been suggested to explain the cause of friction reduction in ultrasonic tactile displays; [Watanabe and Fukui, 1995] proposed that the friction reduction is due to the formation of a squeezed film of air between fingerpad and the surface. Alternatively, it has been suggested that, when a surface vibrates at an ultrasonic frequency, an intermittent mechanical contact develops between fingerpad and the surface such that the fingerpad bounces on the surface while sliding [Dai et al., 2012, Vezzoli et al., 2017, Sednaoui et al., 2017]. A recent study conducted by [Wiertlewski et al., 2016] using a stroboscope revealed that both mechanisms indeed contribute to the friction reduction. Hence, it appears that the fingerpad bounces on a cushion of squeezed film of air. In electrovibration, an electrostatic force of attraction is produced by applying a voltage signal to the conductive layer of a capacitive touch screen, which increases the friction between its surface and fingerpad [Bau et al., 2010, Shultz et al., 2015]. Ultrasonic actuation can provide a higher variation in friction as compared to the electrostatic actuation, while the rendering bandwidth of ultrasonic devices is limited due to its resonating nature [Meyer et al., 2014].

Friction modulation techniques can potentially display a variety of tactile stimuli on the interaction surface of touch-enabled devices. For example, periodic modulation of friction magnitude between two different levels generates a feeling of textured surfaces [Biet et al., 2008b, Biet et al., 2008a, Meyer et al., 2015, Kim et al., 2015, Kalantari et al., 2016, Vezzoli et al., 2016, Vardar et al., 2017b, Vardar et al., 2017a, Rekik et al., 2017, Friesen et al., 2018, Bernard et al., 2018]. Alternatively, data-driven techniques can be used for more realistic rendering of virtual textures [Ben Messaoud et al., 2016, Ilkhani et al., 2017, Jiao et al., 2018, Osgouei et al., 2018]. Moreover, tactile rendering of 3D virtual shapes or bumps is possible by mapping the gradients of a surface to magnitude of friction forces [Kim et al., 2013, Osgouei et al., 2017]. Finally, short duration friction pulses can render virtual edges or haptic-detents, which can improve the user performance in target acquisition tasks [Ware et al., 2014, Zhang and Harrison, 2015, Kalantari et al., 2018], and enhance the design and use of virtual widgets such as buttons and knobs in digital user interfaces [Giraud et al., 2013, Emgin et al., 2018].

1.1 Problem Definition and Approach

In order to effectively use friction modulation techniques, it is important to understand our tactile perception of change in friction and contact mechanics behind it. Although, the earlier studies have investigated the contact mechanics of friction [Adams et al., 2007, André et al., 2009, Derler et al., 2009, Pasumarty et al., 2011, Adams et al., 2013, Delhaye et al., 2014, Delhaye et al., 2016, Sednaoui et al., 2015, Sednaoui et al., 2017] and our perceptual ability to discriminate two different surfaces based on friction [Smith and Scott, 1996, Gueorguiev et al., 2016, Samur et al., 2009], the number of studies investigating the intermittent contact mechanics during a change in friction on a touch surface is very limited [Cornuault et al., 2015, Messaoud et al., 2016a, Saleem et al., 2017, Vardar et al., 2017b]. Similarly, the factors affecting our tactile perception of this change have not been investigated in depth yet [Messaoud et al., 2016a, Saleem et al., 2017, Vardar et al., 2017b, Gueorguiev et al., 2017b, Monnoyer et al., 2017]. Moreover, there is a need to understand how consecutive changes in friction (in the form of virtual textures) affect our tactile perception. In this regard, tactile discrimination and roughness perception of textures are principle aspects that are extensively investigated for real textures, and the underlying perceptual mechanisms are well-established [Taylor and Lederman, 1975, Lederman, 1983, Morley et al., 1983, Sathian et al., 1989, Connor et al., 1990, Connor and Johnson, 1992, Hollins and Risner, 2000, Nefs et al., 2001, Yoshioka et al., 2001, Cascio and Sathian, 2001, Smith et al., 2002, Lawrence et al., 2007, Weber et al., 2013, Sutu et al., 2013, Kocsis et al., 2013, Drewing, 2016]. However, corresponding studies for virtual textures are limited, particularly the ones displayed by friction modulation techniques [Biet et al., 2008a, Smith et al., 2010, Meyer et al., 2015, Kim et al., 2015, Vardar et al., 2017b, Gueorguiev et al., 2017b, Friesen et al., 2018, Bernard et al., 2018]. In particular, there is no in-depth study exploring the roughness perception of virtual textures displayed by ultrasonic actuation.

The first aim of this thesis is to investigate the relation between our tactile perception of friction change and the underlying contact mechanics during sliding. We have conducted psychophysical experiments to evaluate human tactile perception of friction change (called edges in the text) for rising friction (RF) and falling friction (FF), owing to the huge contrast in perception between them reported for pressing-finger [Monnoyer et al., 2016]. First, we measured the detection thresholds under the experimental conditions of RF and FF for sliding-finger and pressing-finger (no intentional sliding). Then we investigated the intensity scaling of friction change for sliding-finger. We performed intensity scaling experiments at different vibration amplitudes (V_{amp}) above the threshold value estimated in the first experiment, finger velocities (f_v), transition times (t_r^{amp}), and mean normal forces ($\overline{F_n}$). Here, the transition time (t_r^{amp}) is defined as the duration in which the vibration amplitude is linearly increased from zero to the desired value (V_{amp}) or vice-versa. Hence, transition time affects the slope of the friction change (e.g. longer transition time indicates slower change in friction).

In the second part of thesis, we explored the tactile perception of virtual textures in the form of periodic square gratings at macro-scale, rendered on a glass surface using the ultrasonic actuation technique. We first investigated the tactile spatial discrimination threshold for two consecutive changes in friction (called edges in the text) and then for multiple edges (called periodic gratings in the text), since it is important that the tactile stimuli are discriminable distinct in the first place for the estimation of their roughness magnitude. Since friction modulation by ultrasonic actuation cannot render all the spatial cues (such as grating height) necessary for the activation of spatial neural mechanism, we hypothesized that temporal cues are more dominant in roughness perception of virtual gratings. To test this hypothesis, we generated a set of discriminable periodic gratings in different spatial periods and investigated their roughness perception.

1.2 Contribution

In this thesis, we have conducted psychophysical experiments to explore the tactile perception of virtual edges and textures, rendered on a glass surface using ultrasonic actuation.

- We investigated the tactile perception of a step change in friction rendered by a rise in friction (RF) and fall in friction (FF). We showed that RF is perceived more strongly than FF.

- We investigated the spatial discrimination threshold between two consecutive edges rendered with FF followed by RF and vice versa. We showed that two consecutive edges rendered with FF followed by RF are easy to discriminate as compared to vice versa.

- We investigated the tactile discrimination of virtual gratings rendered by a series of edge sequence FF followed by RF (i.e. a series of pulses with high friction on average) and vice versa. We showed that discrimination of virtual gratings is not affected by rendering sequence of the edges.

- We have shown that the roughness perception of virtual periodic gratings (spatial period > 2 mm) is primarily governed by the spatial period, despite missing spatial cues in the direction normal to the touch surface (grating height).

1.3 Thesis Organization

This thesis is organized into five chapters including this chapter.

- Chapter 2 has two main sections. In the first section 2.1, a review of studies investigating the tactile perception of friction and change in friction is presented. In section 2.2, studies investigating the discrimination and roughness perception of real and virtual textures are discussed.

- In chapter 3, the experimental setup used in the thesis is elaborated (section 3.1). Absolute threshold to detect a step change in friction under different rendering conditions is evaluated in section 3.2. Section 3.3 covers intensity scaling experiments of change in friction (virtual edge) under different rendering conditions.

- Chapter 4 investigates the tactile perception of consecutive virtual edges. We are presenting the experiments to evaluate the discrimination of two consecutive virtual edges in section 4.1, while the experiments to evaluate the spatial threshold to discriminate virtual periodic gratings are covered in section 4.2. In section 4.3, we are investigating roughness perception of virtual periodic textures.

- The key results of the thesis, and future directions of research are discussed in chapter 5.

Chapter 2

BACKGROUND

2.1 Perception of Friction

2.1.1 Friction on Real Surfaces

The earlier studies in tribology literature show that friction between skin and a smooth glass surface is mainly governed by interfacial interaction (adhesion), while the contribution due to viscoelastic deformations is reported to be low. In case of a smooth surface, increasing the normal force increases tangential force, while the coefficient of friction decreases [Adams et al., 2007, André et al., 2009, Derler et al., 2009, Delhaye et al., 2014, Delhaye et al., 2016]. [André et al., 2009] reported that the effect of normal force on friction coefficient is valid below 3.5 N only. Similarly, the contribution in friction due to viscoelastic deformations decreases rapidly with an increase in normal force, as reported by [Derler et al., 2009]. The friction between a smooth surface and fingertip also varies with moisture, lipids/water ratio, occlusion time, finger velocity, and fingertip roughness [André et al., 2009, Pasumarty et al., 2011, Adams et al., 2013, Cornuault et al., 2015, Delhaye et al., 2016].

Friction plays an important role in human perception of surface features. The ability of humans to discriminate smooth surfaces based on friction was studied by [Smith and Scott, 1996]. They found that the subjects could identify microscopically smooth surfaces with a great accuracy using active touch. Although, the friction coefficients of the surfaces used in their study were very low, yet a higher correlation found between the estimated friction and the measured one. [Smith et al., 2002] investigated the role of friction and tangential force in tactile perception of roughness using linear gratings. They found a positive correlation between friction and roughness perception, however rate of change in tangential force correlated better with roughness estimates. Friction is also important in the discrimination of wet and dry surfaces. [Chen et al., 2009] found that the subjects perceived a surface as dry if the friction and compliance of the surface were low. The above studies suggest that friction is indeed very important in tactile perception. Nonetheless, a recent study showed that two surfaces can be perceived different during tactile exploration, even though they have the same frictional properties, due to the difference in molecular interactions between finger and the surfaces [Gueorguiev et al., 2016].

2.1.2 Friction on Ultrasonically Actuated Surfaces

In an experimental study investigating friction reduction on an ultrasonically actuated plate [Sednaoui et al., 2015], the authors observed that coefficient of friction reduces as vibration amplitude is increased, as expectedly, but there was a limit in which no further improvements could be achieved. Moreover, the change in friction was small for higher normal forces and at values higher than 1 N, there was in fact no perceivable change. Their results also showed that the finger velocity affects the friction coefficient at lower normal loads. On the other hand, [Sednaoui et al., 2017] reported that reduction in friction coefficient using ultrasonic vibrations depends on exploration velocity (tested at 20, 40, and 80 mm/s) but independent of normal force (tested at 0.2, 0.5, and 0.75 N). [Cornuault et al., 2015], have investigated the friction contrast on real and ultrasonically actuated surfaces. They found that the resulting contrast in friction depends on moisture and fingertip roughness, while no correlation was found between fingertip curvature and the spatial period of the ridges in finger skin.

There are very few studies in literature on friction perception during sliding on ultrasonically actuated surfaces. [Samur et al., 2009] have conducted discrimination experiments to evaluate the minimum detectable difference in friction using the tactile pattern display (TPad). The subjects were presented with two stimuli in sequential order and asked to identify the stimulus with higher friction. An average JND of

18% was reported for the friction difference. This study shows the ability of humans to discriminate two surfaces based on friction, but how humans perceive a change in friction cannot be ascertained. In this regard, [Messaoud et al., 2016a] have evaluated the subjects' performance in detecting a change in friction. Their results showed that the detection rate improves at lower inherent friction between finger and surface, as well as lower finger velocity of 5 mm/s compared to 20 mm/s. They also found that the detection rate is best correlated to friction contrast and a contrast greater than 0.19 is always detectable. It is shown in [Saleem et al., 2017] that rate of change in tangential force is best correlated with the detection rate of friction change. [Gueorguiev et al., 2017b] investigated the tactile perception of ultrasonic square signals displayed by friction modulation and observed that subjects could differentiate between two ultrasonic signals if the duration and transition time are extended by 2.4 and 2.1 ms, respectively. In another experiment, they found that if the duration between two pulses was shorter than 50 ms, subjects perceived them as a single pulse. In [Gueorguiev et al., 2017a], authors have evaluated the threshold to detect two friction reductions of 100 ms duration, rendered 3 mm apart, using three different ultrasonically actuated surfaces made of aluminum, polypropylene and polyurethane. The rise time of vibration amplitude was controlled at 1.5 ms. The surfaces were passively scanned under the finger at 20 mm/s, while normal force was maintained at 0.7 N. They conducted threshold experiments and measured the vibration thresholds at 75% JND as 0.17, 0.23, 0.27 µm for aluminum, polypropylene and polyurethane, respectively. Furthermore, the detection rate was found to correlate well with the ratio of reduction in tangential force to pre-stimulation tangential force.

Apart from the studies on sliding-finger, it has been shown that a click effect, as in key press, can be created by reducing the friction as the user presses on an ultrasonically actuated touch surface [Tashiro et al., 2009,Monnoyer et al., 2016,Monnoyer et al., 2017,Saleem et al., 2017]. [Tashiro et al., 2009] have rendered the feeling of buckling and restitution of mechanical buttons using Langevin-type ultrasonic transducer. They argued that the perception of button press and release are due to momentary slippage of the finger over the surface, which occurs when the friction of the surface is reduced by ultrasonic actuation. Unlike [Tashiro et al., 2009], [Monnoyer et al., 2016] argued that the feeling of click occurs due to a sudden release of stress at the fingertip, which is accumulated when the friction of surface is high. Recently, it has been shown that there is an optimal value of finger impedance that leads to a stronger perception of haptic click effect [Monnoyer et al., 2017]. Moreover, the rate of change in normal force has been reported to play an important role in perception of click effect [Saleem et al., 2017].

2.2 Perception of Textures

Most of the surfaces that we touch and interact in our daily life have complex topographies which make them difficult to analyze in tactile perception studies. For this reason, surfaces with periodic topographies like raised-dots and linear gratings have been typically preferred in earlier studies investigating the discrimination and roughness perception of periodic macro-textures, which are discussed below in detail.

2.2.1 Real Textures

Effect of Topography

Several studies have shown that perceived roughness increases with groove width, and decreases with ridge width for linear gratings [Taylor and Lederman, 1975, Lederman, 1983, Morley et al., 1983, Sathian et al., 1989, Yoshioka et al., 2001, Cascio and Sathian, 2001, Lawrence et al., 2007]. However, the effect of ridge width on our tactile perception is less significant than that of groove width [Sathian et al., 1989, Drewing, 2018]. Lederman [Lederman, 1983] observed an increase in perceived roughness with groove width when spatial period or groove to ridge width ratio was kept constant (0.875 mm and 50%, respectively). Yet, the range of spatial periods investigated in [Lederman, 1983] was narrow (0.12 to 1 mm). For a wider range up to 8.5 mm, roughness perception still increases with groove width, but eventually saturates at larger groove widths [Lawrence et al., 2007]. For raised-dots made of cylinders and cones, roughness perception decreases with increasing diameter of dots [Connor et al., 1990, Blake et al., 1997, Tymms et al., 2018]. On the other hand, different trends have been reported in the literature for dot spacing; [Connor et al., 1990] observed that roughness perception follows an inverted U-shaped trend for increasing dot spacing, with a peak value around 3 mm, though [Meftah et al., 2000] reported a monotonic increase in perceived roughness over a similar range. [Sutu et al., 2013] elucidated that inverted U-shape trend in roughness perception is valid only if height of dots is low. This allows the fingerpad to contact the base surface between the dots more easily, resulting in a drop in perceived roughness. However, for higher dots, increase in roughness perception with increasing dot spacing was monotonic. [Drewing, 2016] has extended the work of [Sutu et al., 2013] by investigating the roughness perception of linear gratings with a lower height for spatial periods varying from 0.5 to 10 mm. He observed an inverted U-shape trend in roughness perception for sinusoidal gratings as well, and modest decrease for square gratings at larger spatial periods.

[Sutu et al., 2013] have observed an interesting relation between discrimination threshold (Weber fraction) and roughness perception for dotted surfaces. Their results showed that the Weber fraction was around 4-5% for smaller dot spacing (corresponding to the ascending half of U-shaped roughness function), irrespective of the dot height. On the other hand, Weber fraction was significantly higher (8-12%) for dots with lower height and larger dot spacing (corresponding to the descending half of U-shaped roughness function). Although, they reported an increase in Weber fraction for higher raised-dots, the effect was less significant. A similar Weber fraction of 5% was also reported by [Morley et al., 1983] for the discrimination of linear gratings of square shape, and 0.8 and 1 mm in spatial period. [Nefs et al., 2001] investigated the sinusoidal linear gratings and observed a decrease in Weber fraction with increasing spatial period (12, 6.3, and 6.4% for spatial periods of 2.5, 5, and 10 mm, respectively). Furthermore, they found no significant effect of grating height on discrimination of spatial period, but significant effect of spatial period on discrimination of height. [Kocsis et al., 2013] investigated the effect of texture profile on height discrimination of linear gratings and found no significant difference between sinusoidal and triangular gratings.

Effect of Contact Forces

Earlier studies have shown that perceived roughness increases with increasing normal force [Lederman and Taylor, 1972, Lederman, 1974, Lederman, 1983]. [Taylor and Lederman, 1975] showed that the roughness perception of linear gratings correlates positively with the static deformation of fingerpad under normal loading. The reliable prediction of perceived roughness without even considering the dynamics of movement suggests that the friction coefficient should have no effect, which was experimentally confirmed by the authors in the same study [Taylor and Lederman, 1975]. However, more conclusive results on this topic were presented by [Smith et al., 2002] later. They investigated roughness perception by varying spatial period between 1.5 to 8.5 mm, and altering friction coefficient by coating the surface with liquid soap. They found a significant but inconsistent correlation between roughness perception and friction coefficient for all subjects, while the roughness perception was best correlated with the rate of change in tangential force.

Neural Mechanism

It has been shown that the discrimination and roughness perception of macro-textures are not affected by finger velocity [Lederman, 1974, Lederman, 1983, Hollins and Risner, 2000]. [Meftah et al., 2000] observed an increase in roughness perception by increasing dot spacing in the direction transverse to finger motion. These findings strongly argue against the temporal mechanism behind the perception of macro-textures. Furthermore, a series of combined psychophysical and neurophysiological experiments were conducted to understand the underlying neural mechanism behind roughness perception of macro-textures [Sathian et al., 1989, Connor et al., 1990, Connor and Johnson, 1992, Blake et al., 1997, Yoshioka et al., 2001]. The results showed that roughness perception is encoded spatially, and there is a linear relation between perceived roughness and spatial variation in firing rates of SA1 afferent fibers. However, contribution of temporal cues in the discrimination and roughness perception of macro-textures cannot be fully ignored. [Morley et al., 1983] have noted a drop in discrimination performance (Weber fraction increased from 5% to 10%) when the finger is pressed on the surface without sliding (i.e. static contact). This is because finger movements provide additional vibration cues which enhance the perception. Similarly, [Kocsis et al., 2013] have observed an increase in discrimination performance of linear gratings, if explored with a rigid probe. This was due to the efficient transfer of vibration cues as a result of an increase in the contact area (i.e. holding the probe increases the area in contact with the hand, as compared to a fingerpad exploring the surface). [Cascio and Sathian, 2001] have observed a significant influence of temporal frequency on the discrimination and roughness perception of linear gratings for varying ridge width, but not for groove width. They also calculated the mean firing rates for SA1, PC, and RA afferent fibers, and found that decreasing (increasing) trend in roughness perception for increasing ridge width (groove width) was best correlated with mean firing rate of PC (SA1) afferent fibers.

2.2.2 Virtual Textures

Roughness perception of periodic virtual textures was investigated using force feedback devices in [Drewing et al., 2004, Kornbrot et al., 2007, Unger et al., 2011, Klatzky and Lederman, 2006, Lederman et al., 2006, Smith et al., 2010], and the results suggest significant influence of virtual probe diameter. For a point-probe (having an infinitely small diameter) exploring virtual gratings, [Kornbrot et al., 2007] reported a decrease in perceived roughness with increasing spatial period varied from 0.7 to 2.7 mm. [Unger et al., 2011] observed a flat trend in roughness perception up to 2 mm, followed by a drop at larger spatial periods for a point-probe. On the other hand, they observed a monotonic increase in perceived roughness for increasing spatial period from 1 to 6 mm for spherical virtual probes having a diameter varying from 0.25 to

1.5 mm. Similarly, for dotted surfaces, a continuous decrease in perceived roughness was observed for a point-probe [Drewing et al., 2004], and inverted U-shaped function for the spherical-probes [Unger et al., 2011]. Unger et al. noted that the peak value of perceived roughness shifts towards higher periods with increasing probe diameter, similar to real textures [Klatzky and Lederman, 1999, Klatzky et al., 2003].

It is important to note here that force feedback devices have been utilized in the above studies, which are capable of resolving 3D forces. Hence, a change in surface topography can be easily simulated. [Klatzky and Lederman, 2006, Lederman et al., 2006] investigated the roughness perception of periodic gratings rendered by a haptic mouse that can change sliding resistance only. They found that roughness increases with spatial period (varying from 0.08 to 8 mm) if ridge to groove width ratio was kept constant. Further analysis showed that ridge width had a dominant effect, while the effect of groove width was negligible. [Smith et al., 2010] rendered periodic gratings (varying from 1.5 and 8.5 mm in spatial period) using a force feedback device which could only display tangential forces resisting to the planar movements. Unlike [Klatzky and Lederman, 2006], they observed a decrease in roughness perception when spatial period was increased, and a strong influence of friction coefficient and tangential force on roughness perception.

The discrimination and roughness perception of periodic gratings, rendered on a surface using friction modulation techniques have been far less studied. [Vardar et al., 2017b] investigated the roughness perception of periodic gratings displayed by electrovibration. They compared four waveforms; sine, square, triangular and saw-toothed waves with spatial period varying from 0.6 to 8 mm. The width of periodic high friction regimes (analogous to ridge width) was taken as 0.5 mm, while that of the low friction ones (analogous to groove width) was varied. The finger velocity was controlled indirectly by displaying a visual cursor moving at 50 mm/s. The results showed that square waveform was perceived as the roughest, while there was no significant difference between the other three waveforms. The perceived roughness decreased with increasing spatial period in general, though a modest U-shaped trend was observed with a peak value around 2 mm. They also reported that the roughness perception of periodic gratings correlates best with the rate of change in tangential force, similar to the real gratings [Smith et al., 2002]. The discrimination of periodic gratings, rendered on a touch surface by ultrasonic actuation was investigated in [Biet et al., 2008a]. The surface was vibrated at a frequency of 30 kHz with an amplitude of 1.1 µm. Four standard and eight comparison gratings in square waveform were rendered. The width ratio of high to low friction regimes was always kept constant. The finger velocity was not controlled. The results showed that the difference threshold (JND) increases with spatial period (0.2, 0.32, 0.47 and 0.8 mm for spatial period of 2.5, 3.5, 5 and 10 mm, respectively). Unlike real gratings [Nefs et al., 2001], Weber fraction remained almost constant (varied between 8 and 10 %).

Chapter 3

PERCEPTION OF A STEP CHANGE IN FRICTION

Ultrasonic actuation can display a variety of tactile stimuli by modulating the friction of the surface. Hence, understanding the perception of a change in friction is important. In this chapter, we are investigating the tactile perception of a step change in friction rendered by ultrasonic actuation.

3.1 Experimental Setup

The tactile display used in our study is a 100×60 mm^2 glass surface of 1.4 mm thickness. We actuate it at 26.9 kHz using two piezoelectric patches (7BB-35, Murata Manufacturing) and a high voltage amplifier (PZD700A M/S, Trek). At the selected vibration mode, the distance between the nodal lines is approximately 11 mm, creating an area of 11×60 mm^2 between two nodal lines for tactile exploration as shown in Figure 3.1. A force sensor (Nano17 Titanium, ATI Industrial Automation) capable of measuring up to 8 N with a resolution of 1.5 mN is used to record the normal and tangential forces acting on finger during the experiments. To acquire the vibration amplitude during contact interactions, a small piezoelectric patch (FT-10.5T, Kepo Electronic) is used as a sensor. We have used an analog RMS-circuit to record the vibration amplitude at a lower sampling rate. The piezoelectric sensor is calibrated by a Laser Doppler Vibrometer (LDV) (OFV-551, Polytec). To record the force and vibration amplitude simultaneously, we have used two data acquisition cards (PCI-6034E, National Instruments) and (PCIe-6321, National Instruments) running at 5k samples/seconds. To control finger velocity in a pseudo-active manner (f_v) during the experiments, we used a linear stage as shown in Figure 3.2.

To create different tactile effects on the touch surface using ultrasonic actuation technique, vibration amplitude (V_{amp}) and transition time (t_r^{amp}) are used as the main control parameters. Finger damping during contact may cause fluctuations in V_{amp} and an active control might be required [Giraud et al., 2013, Messaoud et al., 2016b]. However, in our experiments, the recorded vibration amplitude showed reasonable precision and accuracy without any active control, as depicted in Figure 3.3.

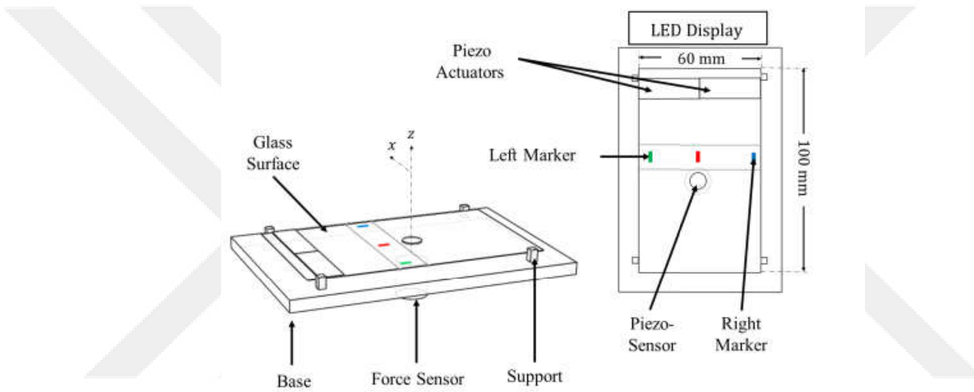

Figure 3.1: Illustration of variable friction tactile display used in the study.

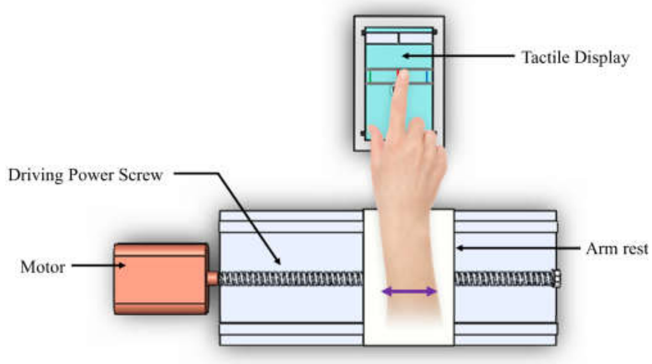

Figure 3.2: Illustration of experimental setup used for controlling f_v.

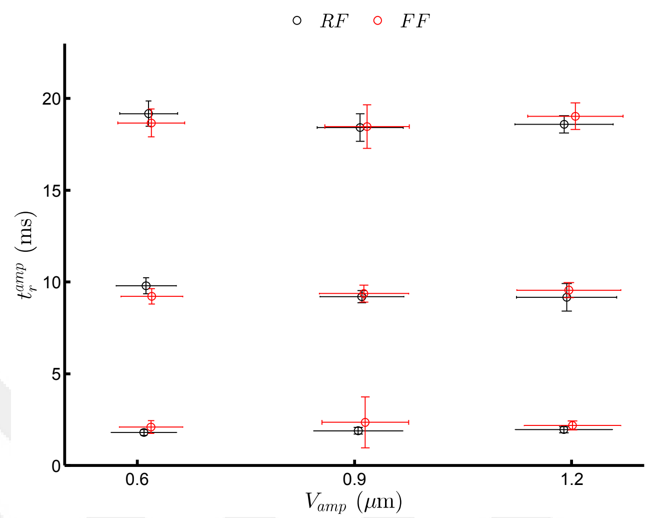

Figure 3.3: Means and standard deviations for V_{amp} and t_r^{amp} recorded during the experiments. Tick values on horizontal and vertical axes are the desired values for V_{amp} and t_r^{amp}, respectively

3.2 Threshold Estimation Experiments

The first part of the chapter focuses on finding the smallest change in friction that humans can detect. We measured the perceptual thresholds for a) sliding-finger and b) finger pressed on the surface (no intentional sliding).

3.2.1 Experimental Design

The threshold estimation experiments were conducted using the method of constant stimuli [Jones and Tan, 2013]. There were two experimental conditions; rising friction (RF) and falling friction (FF). We rendered each condition at different vibration amplitudes (V_{amp}) by altering the actuation voltage applied to the piezoelectric patches. The transition time (t_r^{amp}) was chosen as 2 ms in these experiments. The touch surface was actuated at 10 different vibration amplitudes (corresponding to 10 different voltage levels) varying from 0 to 0.6 µm in sliding-finger experiment, and from 0 to 1.2 µm in pressing-finger experiment. Each stimulus was repeated 10 times, hence each subject completed 200 trials (2 conditions × 10 different voltage levels × 10

Table 3.1: Vibration amplitude (µm) at mean threshold levels

	Friction Change	50 %	75 %
Sliding Finger	RF	0.21±0.02	0.27±0.02
	FF	0.22±0.02	0.30±0.02
Pressing Finger	FF	0.50±0.04	0.78±0.06

repetitions). The trials were displayed in a random order, while the same order was displayed to each subject.

3.2.2 Procedure

In sliding-finger experiment, the subjects explored the surface from left to right only. The subjects were instructed to synchronize their finger velocity with a visual cursor moving with a velocity of (50 mm/s). We changed the friction as the subjects' finger crossed the mid-point of the exploration region, which was detected by an IR-frame (see "RED" mark in Figure 3.1). The subjects were asked to respond to the following question by saying YES/NO; "Did you feel any tactile effect?"

In pressing-finger experiment, the subjects were asked to press their finger on the touch surface marked in "RED". Therefore, the spatial location where we changed the friction was same for both threshold estimation experiments. We changed the friction when the normal force (F_n) applied by finger exceeded 0.3 N. A LED display turned ON to indicate that there was a change in tactile stimuli and then subjects were asked to respond to the following question by saying YES/NO; "Did you feel a click?"

Ten subjects participated in the threshold estimation experiment (7 males, 3 females, average age of 27±3). The subjects read and signed the consent form before the experiments. The form was approved by Ethical Committee for Human Participants of Koc University.

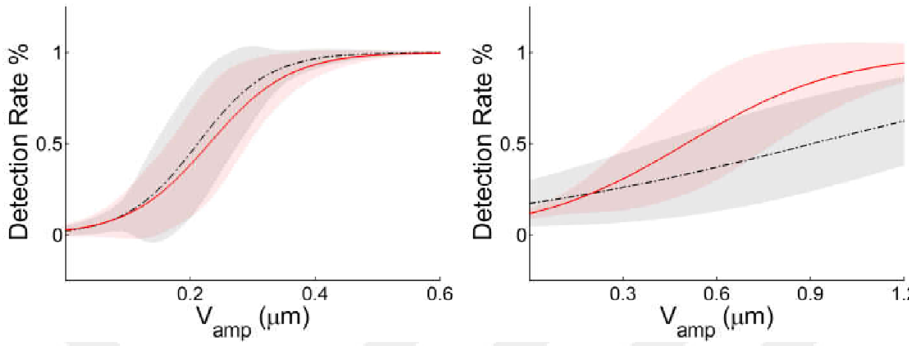

(a) (b)

Figure 3.4: Psychometric responses for threshold experiments. (Black-dotted: RF, red-solid: FF). Shaded region depicts standard deviation in detection rate. (a) Sliding-finger and (b) finger pressed on the surface (no sliding).

3.2.3 Results

We fitted a logistic function to the mean response of each subject for RF and FF, separately. Then, an average curve for all subjects for RF and FF was constructed from the individual curves and threshold values were reported based on those average curves. The results of sliding-finger experiment showed that subjects' perception of RF and FF was quite similar (Figure 3.4(a)), and followed a typical psychometric response ($R^2 = 0.98$). The paired t-test unveiled that the difference between RF and FF was not significant ($p = 0.08$). The results of the pressing-finger experiment are shown in Figure 3.4(b). We found that the response for FF followed a typical psychometric behavior ($R^2 = 0.99$), whereas RF was not perceived as a click and curve fit was poor ($R^2 = 0.5$). The paired t-test showed that the difference between RF and FF was significant ($p < 0.001$). Our results are in line with the recent literature [Monnoyer et al., 2016]. The vibration amplitudes (V_{amp}) for the mean detection rates of 50 and 75 % are given in Table 3.1 (For pressing-finger experiment, data for FF condition was reported only). For further details on our threshold experiments, the readers are referred to [Saleem et al., 2017].

The threshold experiments showed that RF and FF were perceived equally when finger was sliding, whereas a pressing-finger could only detect FF. Moreover, the perceptual threshold for FF in pressing-finger experiment was twice the value measured for the sliding-finger experiment. The threshold experiment provided us valuable information about the tactile limits. However, the ability of humans to estimate the intensity of friction change cannot be ascertained from a threshold experiment. In the next section, we explore how subjects rate the intensity of friction change under different experimental conditions.

3.3 Intensity Scaling Experiments

In the second part of the chapter, we assessed the subjects' perception of change in friction intensity during sliding. We have chosen our vibration amplitudes (V_{amp}) significantly above the detection levels estimated for the sliding-finger in the first experiment. We altered finger velocity (f_v), transition time (t_r^{amp}), and the mean normal force applied to the surface ($\overline{F_n}$) in a controlled manner to investigate if they cause any bias in intensity scaling. The travel distance of the linear stage was 40 mm during the experiments

3.3.1 Experimental Design

There are three experiments in this part. In the first experiment (EXP-1), t_r^{amp} was kept constant at 2 ms while f_v and V_{amp} were varied. Hence, there were a total of nine rendering conditions (f_v = 10, 40, 70 mm/s) and V_{amp} = (0.6, 0.9 and 1.2 µm). The values selected for f_v are in line with the values reported in earlier tactile exploration studies [Sednaoui et al., 2017, Messaoud et al., 2016a, Gueorguiev et al., 2017a, Ramalho et al., 2013, Tanaka et al., 2014]. In the second experiment (EXP-2), f_v was kept constant at 40 mm/s while t_r^{amp} and V_{amp} were varied. Hence, there were again nine rendering conditions (t_r^{amp} = 2, 10, 20 ms) and V_{amp} = 0.6, 0.9, 1.2 µm). The normal force was not controlled in EXP-1 and EXP-2. In the third experiment (EXP-3), the t_r^{amp} and f_v were kept constant at 2 ms and 40 mm/s respectively, while V_{amp} and the normal force applied by the subject ($\overline{F_n}$) were varied. The experiments were conducted under "low" and "high" normal forces. We observed that the subjects applied an average normal force of 0.3±0.15 N in EXP-1 and EXP-2. For this reason, in EXP-3, the subjects were instructed to keep their finger load below 0.15 N under the "low" condition, while they were asked to apply normal forces greater than 0.45 N under "high" condition. Hence, there were a total of 6 rendering conditions (3 $V_{amp} \times 2 \overline{F_n}$). In all the experiments, each condition was repeated 10 times for rising friction (RF) and falling friction (FF). Hence, there were a total of 180 trials in EXP-1 and EXP-2, and 120 trials in EXP-3. The trials were randomized while the same randomization pattern was used for all subjects.

3.3.2 Procedure

The subjects were given a brief presentation and a training session to familiarize themselves with the setup. They were asked to put their arm over the linear stage and place their finger on the left marker (see Figure 3.1). We changed the friction when subjects' finger crossed the "RED" marker in the middle during sliding. The motion starts from the left marker and ends at the right marker and the subjects were asked to rate the difference in friction using a Likert scale varying from 1 to 7 ("1" represents the weakest change while "7" is the strongest). The next trial starts from the right marker and ends at the left marker and this process repeats itself. The trials were randomized such that each rendering condition displayed equally for the movements from left to right and right to left. We used a computer fan to continuously blow air over the touch surface to minimize the undesirable effects of moisture. Moreover, the subjects were instructed to lift their finger up at the end of each trial to release accumulated stresses. A white noise was played through active noise canceling headphones to prevent perceptual bias due to any auditory noise. In EXP-1 and EXP-2, the subjects were instructed to press the surface gently, like touching the surface of a mobile phone or a tablet. There was one minute break after every 36 trials, during which the finger of subject was cleaned with alcohol. In EXP-3, we displayed a reference value (i.e. desired value) for the normal force to the subjects

Table 3.2: The number of subjects who perceived rising and falling friction differently

	G_{RF}	G_{FF}	G_N	$Total$
EXP-1	6	1	2	9
EXP-2	5	1	4	10
EXP-3	5	1	3	9

through a GUI (0.15 N for "low" force and 0.45 N for "high" force). The reference force was changed after every 12 trials, preceding a break of one minute (note that we did not change the reference force after each trial because our preliminary experiments showed that the subjects could not adapt well to this procedure).

Eleven subjects participated in the experiments (9 males, 2 females, average age of 27±4). The subjects read and signed the consent form before the experiments. The form was approved by Ethical Committee for Human Participants of Koc University.

3.3.3 Results

First, we normalized the scores (S_n) of each subject to vary between zero and one. We observed inconsistent responses for a few subjects, perhaps due to misunderstanding of the task or lack of concentration during the task. Therefore, we measured within-subject variability by computing coefficient of variation (CV) and then calculated interquartile range (IQR) in CVs for all subjects. The data of subjects with CVs more than 1.5 $\times$ IQR above the upper quartile were rejected (as a result, the data of 2/11 subjects in EXP-1 and EXP-3, while 1/11 subject in EXP-2 was rejected). The results showed that subjects scored RF higher than FF as shown in Figure 3.5. Nonetheless, this trend was not same among the subjects. We conducted paired t-tests and categorized the subjects in three groups accordingly; a) those who scored RF higher than FF (with $p < 0.05$) are called RF-biased group (G_{RF}), b) those who scored FF higher than RF are called FF-biased group (G_{FF}), and c) those who perceived RF and FF equally ($p \geq 0.05$) are called neutral group (G_N). The number of subjects in each group are listed in Table 3.2.

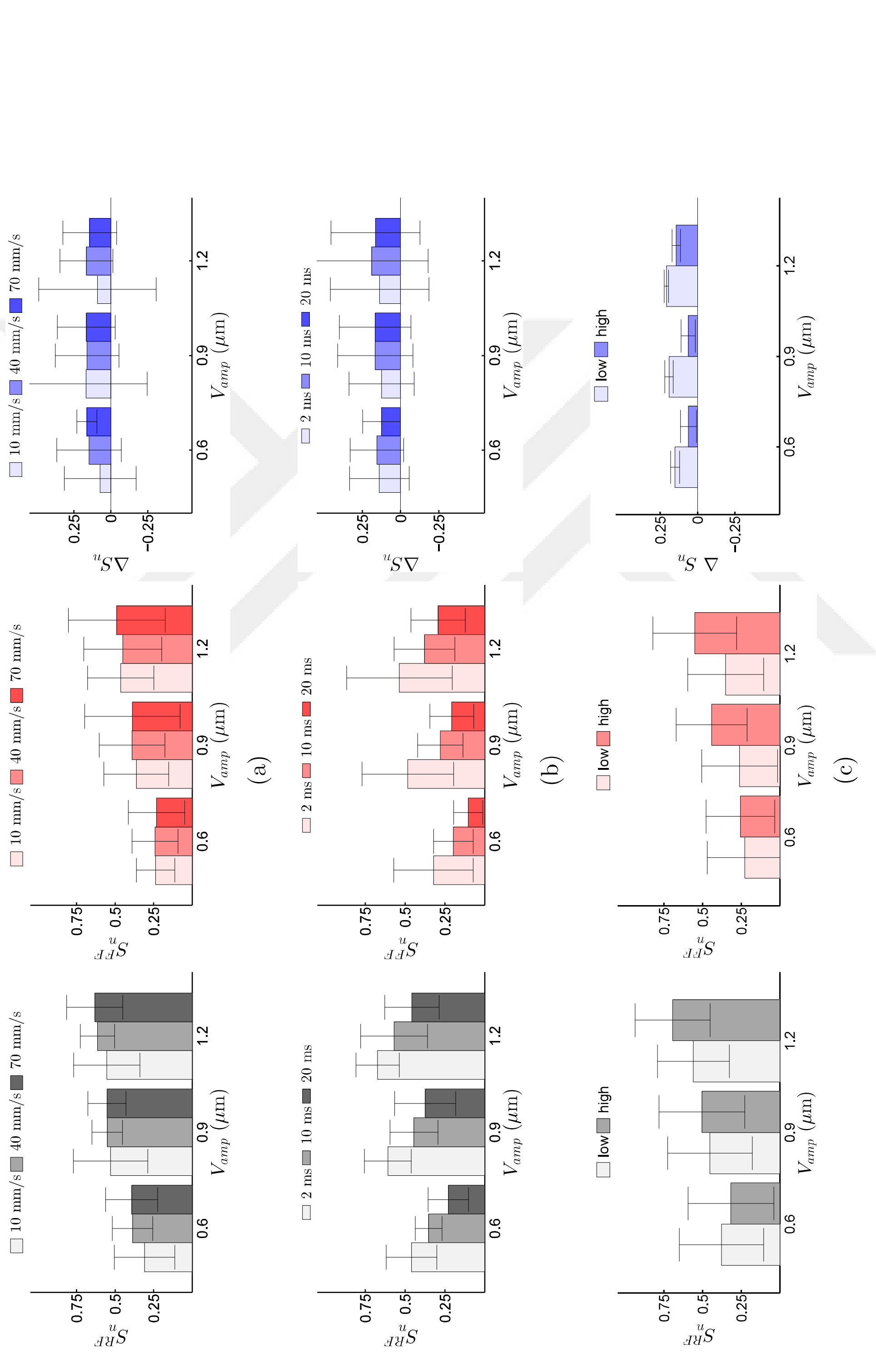

Figure 3.5: Mean scores and standard deviations for intensity scaling experiments; (a) EXP-1, (b) EXP-2 and (c) EXP-3

The results of intensity scaling experiments are summarized below:

- In all experiments, increasing V_{amp} increased S_n as expected.

- In all experiments, average values of S_n for RF was higher than that of FF ($p < 0.01$). Therefore, the difference between scores ($\Delta S_n = S_n^{RF} - S_n^{FF}$) was positive.

- The results of EXP-1 showed that there was no significant effect of f_v on S_n.

- In EXP-2, increasing t_r^{amp} decreased S_n. All paired t-tests between S_n values for $t_r^{amp} = 2$, 10, 20 ms returned $p < 0.001$.

- In EXP-3, paired t-test showed that S_n values of subjects were higher under high normal force than those of the low normal force for FF ($p < 0.05$).

- Overall, ΔS_n was not influenced significantly by f_v and t_r^{amp} but its absolute value decreased as $\overline{F_n}$ was increased. (See plots of ΔS_n in Figure 3.5).

3.3.4 Analysis of Forces

Intensity scaling experiments showed that RF and FF were perceived differently by the subjects. To better understand the reasoning behind this, we analyzed the contact forces recorded during the experiments. Before the analysis, the force data was filtered using a low-pass filter with a cut-off frequency of 600 Hz. The cut-off frequency was chosen to cover the sensitivity range of human finger [Fagiani et al., 2012]. For the analysis, we considered a window of data only, which was centered around the transition time and corresponded to the data collected for 70% of the total sliding time. We further sub-divided this window in time domain as elaborated in Figure 3.6 to develop various force metrics (Table 3.3).

Calculating the transition time of force ($t_r^{force} = t_f - t_o$) was challenging due to the variation in contact forces, even at constant stimulation level. To tackle with this problem, t_f is defined as the time when the derivative of tangential force (dF_t/dt)

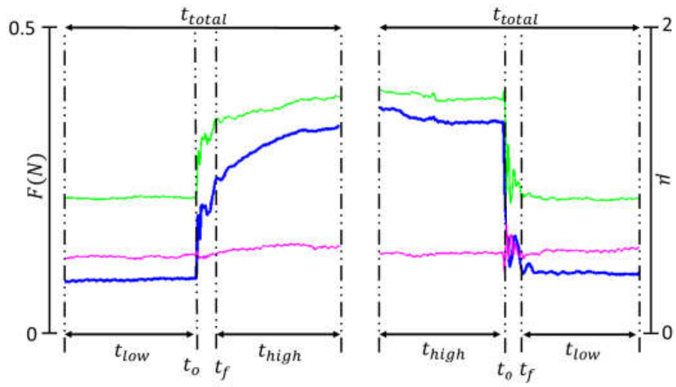

Figure 3.6: An exemplar data window used for the computation of force metrics for RF(left) and FF(right). Blue, magenta and green colored lines represent F_t, F_n and μ, respectively.

Table 3.3: Force metrics, their symbols and descriptions

Force Metric	Symbol	Description
Instantaneous: Tangential Force Normal Force Friction Coefficient	F_t F_n μ	Force in sliding direction, and normal direction. $\mu = F_t/F_n$
Mean: Tangential Force Normal Force Friction Coefficient	F_t^{low}, F_t^{high}, F_t^{mean} F_n^{low}, F_n^{high}, F_n^{mean} μ^{low}, μ^{high}, μ^{mean}	Mean values at t_{low}, t_{high}, t_{total}
Difference: Tangential Force Normal Force Friction Coefficient	ΔF_t ΔF_n $\Delta \mu$	$F_t^{high} - F_t^{low}$ $F_n^{high} - F_n^{low}$ $\mu^{high} - \mu^{low}$
Contrast: Tangential Force Normal Force Friction Coefficient	F_tC F_nC μC	$1 - F_t^{low}/F_t^{high}$ $1 - F_n^{low}/F_n^{high}$ $1 - \mu^{low}/\mu^{high}$
Transition Time: Tangential Force	t_r^{force}	$t_f - t_o$
Rate of change: Tangential Force Normal Force Friction Coefficient	dF_t/dt dF_n/dt $d\mu/dt$	RMS values for time interval of t_r^{force}

Table 3.4: Transition time of tangential force during the experiments at various conditions

	f_v (mm/s)	t_r^{amp} (ms)	$\overline{F_n}$ (N)	t_r^{force} (ms)	
				RF	FF
EXP-1	10	2	-	23±11	22±14
	40	2	-	10±1	6.9±2
	70	2	-	10±1	6.9±2
EXP-2	40	2	-	11±1	7.2±3
	40	10	-	18±3	18±8
	40	20	-	37±7	29±8
EXP-3	40	2	< 0.15	10±2	6±2
	40	2	> 0.45	10±2	6.5±2

decays below 80% of its peak value after t_o, where t_o is defined as the time when the friction change was rendered while the subjects' finger crossed "RED" marker. The values computed for t_r^{force} are shown in Table 3.4. The results showed that, t_r^{force} was significantly higher than t_r^{amp} for both RF and FF, and t_r^{force} in RF was in general higher than that of FF. Moreover, t_r^{force} at low scan speed of 10 mm/s was significantly higher as compared to the typical scan speeds of $f_v = 40$ and 70 mm/s. [Meyer et al., 2014] have also reported a higher force transition time in RF for a lower velocity of 20 mm/s and argued that it is due to slow discharge of squeeze film. Figure 3.9(a) shows that the subjects were successful in attaining and maintaining the desired "low" and "high" normal forces in EXP-3. We investigated the correlation between S_n and normalized force metrics using Spearman correlation (r_s) and the results were checked for the statistical significance level of $p < 0.05$.

Following are the main results gathered from the force metrics and their correlation with S_n:

- It can be seen from Figures 3.7, 3.8, and 3.10 that S_n was correlated with F_tC and dF_t/dt. Results of the correlation analysis (see Table3.5) also supported this observation.

Table 3.5: Force metrics showing highest correlation with S_n

	EXP-1		EXP-2		EXP-3	
	Metric	r_s	Metric	r_s	Metric	r_s
RF	F_tC	0.59	dF_t/dt	0.75	F_tC	0.65
	μC	0.56	t_r^{force}	-0.63	dF_t/dt	0.63
	ΔF_t	0.54	F_tC	0.62	μC	0.63
FF	F_tC	0.67	dF_t/dt	0.81	dF_t/dt	0.59
	μC	0.48	t_r^{force}	-0.79	t_r^{force}	-0.56
	dF_t/dt	0.47	-	-	F_tC	0.4

- The force analysis of EXP-2 showed that F_tC did not change much with t_r^{amp}. Therefore, despite longer t_r^{force}, the contact forces reached a steady-state value within 40 mm of travel distance as shown in Figure 3.8(a) and 3.8(b).
- In EXP-3 , as $\overline{F_n}$ was increased, F_tC reduced, while dF_t/dt and S_n increased (see Figure 3.10).

Table 3.6: Coefficients of linear fit for intensity scaling

	RF				FF			
	c_1	c_2	c_3	R^2	c_1	c_2	c_3	R^2
EXP-1	-0.09	0.86	0.25	0.94 ($p < 0.001$)	-0.018	0.47	0.26	0.89 ($p < 0.001$)
EXP-2	0.04	0.4	0.5	0.97 ($p < 0.001$)	0.02	0.2	0.6	0.93 ($p < 0.001$)
EXP-3	-0.01	0.43	0.65	0.89 ($p < 0.05$)	-0.09	0.4	0.62	0.96 ($p < 0.001$)

The results of all three experiments showed that dF_t/dt and F_tC were the most important metrics in intensity scaling of friction change. In order to find their relative contributions, we fitted a linear model using Matlab function (fitlm) to the normalized scores of subjects in the form of $S_n = c_1 + c_2 \times F_tC + c_3 \times dF_t/dt$ using the normalized values of F_tC and dF_t/dt (see Table 3.6). We found that the contribution of dF_t/dt was more prominent in EXP-2 and EXP-3, while F_tC had a stronger effect in EXP-1.

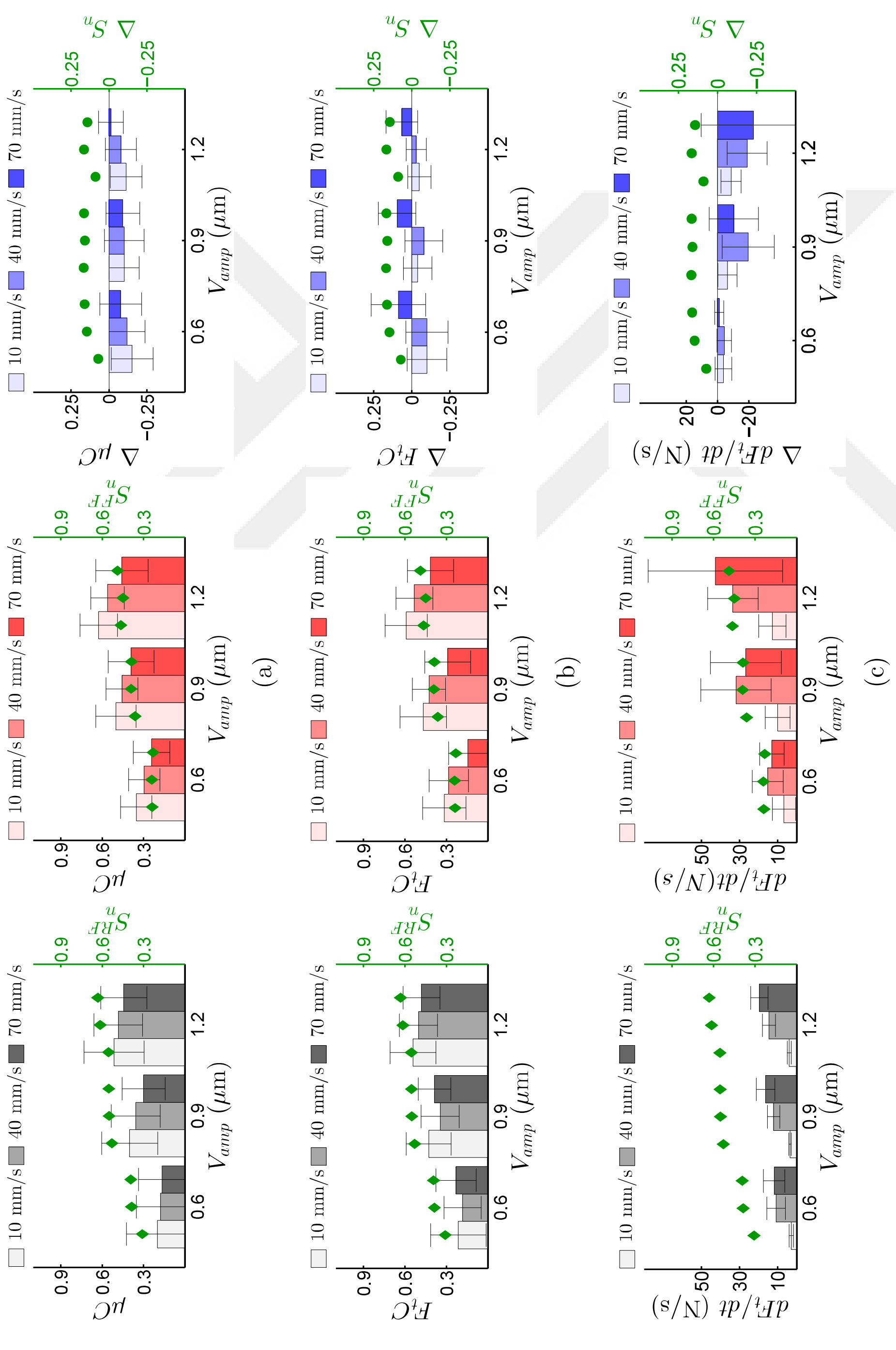

Figure 3.7: Means and standard deviations of various force metrics for EXP-1. The first, second, and third column report the results for RF, FF, and difference between RF and FF, respectively. Green-colored diamonds and circles represent mean values of S_n and ΔS_n, respectively (Refer to the values on the right axis in each plot).

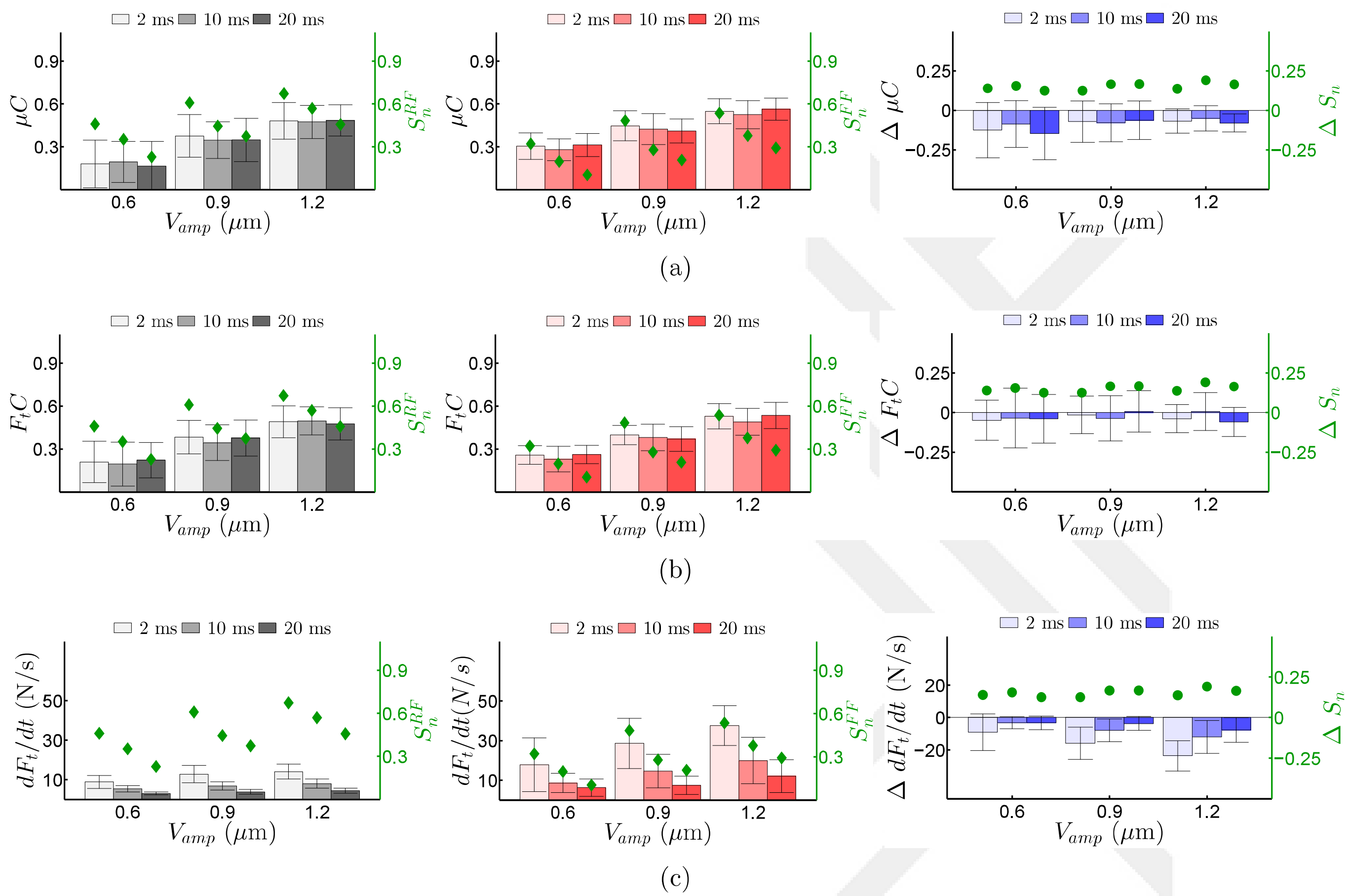

Figure 3.8: Means and standard deviations of various force metrics for EXP-2. The first, second, and third column report the results for RF, FF, and difference between RF and FF, respectively. Green-colored diamonds and circles represent mean values of S_n and ΔS_n, respectively (Refer to the values on the right axis in each plot).

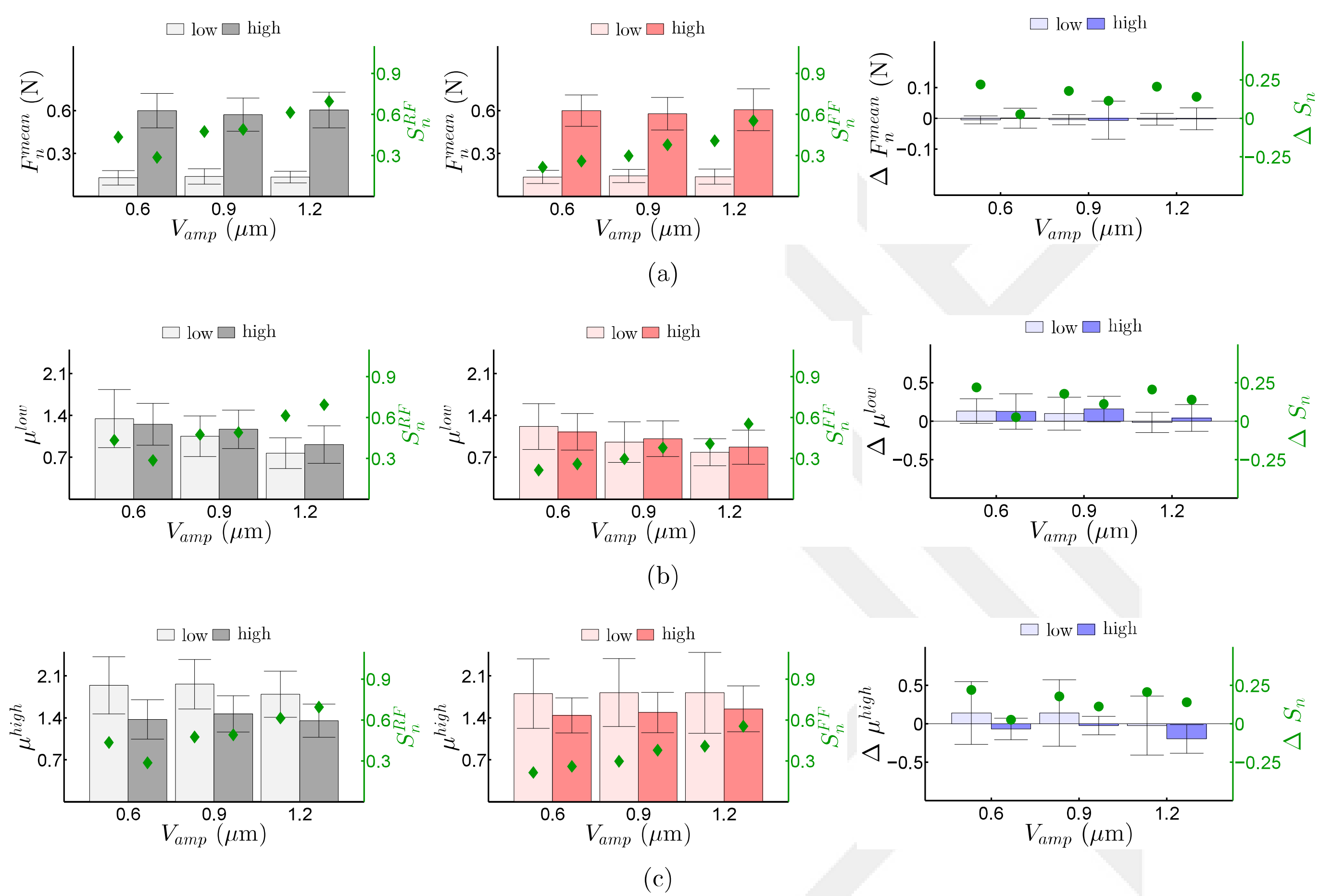

Figure 3.9: Means and standard deviations of various force metrics for EXP-3. The first, second, and third column report the results for RF, FF, and difference between RF and FF, respectively. Green-colored diamonds and circles represent mean values of S_n and ΔS_n, respectively (Refer to the values on the right axis in each plot).

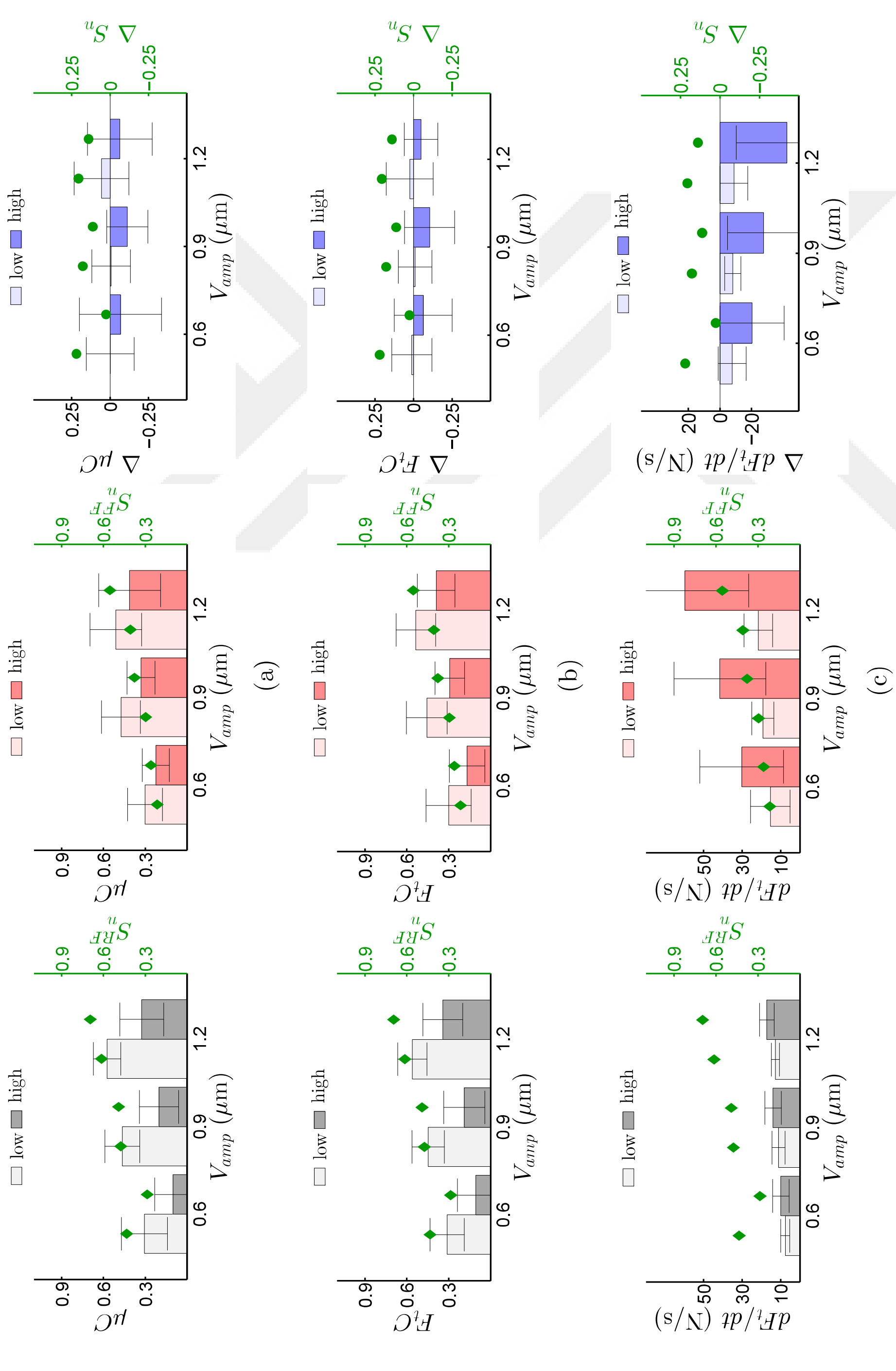

Figure 3.10: Means and standard deviations of various force metrics for EXP-3. The first, second, and third column report the results for RF, FF, and difference between RF and FF, respectively. Green-colored diamonds and circles represent mean values of S_n and ΔS_n, respectively (Refer to the values on the right axis in each plot).

3.4 Discussion

The analysis of contact forces showed that contrast in tangential force (F_tC) and rate of change in tangential force (dF_t/dt) were best correlated with the perceived intensity of friction change (S_n). In fact, S_n can be estimated quite accurately by a linear function of F_tC and dF_t/dt, which suggests that there may be multiple sensory mechanisms involved in the perception of friction change. F_tC causes a difference in magnitude of skin stretch while dF_t/dt is more related to the vibrotaction. We argue that those are the two main mechanisms contributing to our tactile perception of change in friction. However, it is difficult to perform controlled experiments to assess their individual contribution to our perception since they are not easily separable from each other, as argued by [Gueorguiev, 2016]. In the upcoming paragraphs, we discuss the results of each experiment one by one and attempt to justify our argument.

In EXP-1, the finger velocity (f_v) did not affect S_n. The analysis of forces showed that, μC and F_tC slightly decreased, while dF_t/dt increased with increasing f_v (see Figure 3.7). Therefore, the combined effect of F_tC and dF_t/dt resulted in no significant change in S_n as f_v was increased. On the other hand, [Messaoud et al., 2016a] have noted a significantly higher μC at a lower velocity of 5 mm/s as compared to 20 mm/s. Likewise, they observed higher detection rates for friction change at 5 mm/s. The difference in μC reported in their study and ours could be due to a PVC film used in [Messaoud et al., 2016a], while we conducted our experiments on a glass surface. Moreover, μC is known to be affected by amount of moisture and hydrolipid film between fingertip and touch surface [Pasumarty et al., 2011, Cornuault et al., 2015], which were not controlled in either studies.

In EXP-2, S_n decreased when friction was changed smoothly by making t_r^{amp} longer. In other words, when the rate of loading/unloading was higher (shorter transition time), the effect was stronger. We believe that S_n decreased at higher t_r^{amp} because the change in tangential force no longer followed a sharp transition and could not strongly activate mechanoreceptors as discussed in [Vardar et al., 2017a] for electrovibration. A similar perceptual trend was reported for the magnitude estimation of skin stretch applied to human palm in [Guzererler et al., 2016]. On the other hand, [Shull et al., 2010] and [Paré et al., 2002] reported that rate of loading did not affect the magnitude estimates of torsional stretch applied to forearm, and force applied to fingertip, respectively (it is important to note that the loading rates of 0.1, 0.15, and 0.3 N/s used in [Paré et al., 2002] were very low).

In EXP-3, F_tC decreased significantly at high normal force ($\overline{F_n}$), while S_n did not change much. [Derler et al., 2009] reported that the contribution of viscoelastic deformations on the friction decreases as the normal force increases. Similarly, results of EXP-3 showed that increasing $\overline{F_n}$ decreased friction coefficient (μ^{high}) (see Figure 3.9(c)). Interestingly, μ^{low} did not change much with $\overline{F_n}$ as shown in Figure 3.9(b). For this reason, we observed a sharper drop in μC at high $\overline{F_n}$. A similar perceptual effect for normal force was observed in a psychophysical experiment conducted to estimate the magnitude of slip on fingertip [Ho and Hirai, 2017]. The authors argued that the fingertip gets stiffer at higher gripping force (as reported in [Wang and Hayward, 2007]), which results in higher tangential force and magnitude estimates. Similarly, in EXP-3, despite a decrease in F_tC, an increase in dF_t/dt was a clear indication of increased fingertip stiffness.

In sliding experiments performed above the detection threshold, we observed that RF was more strongly perceived than FF, and the difference ($\Delta S_n = S_n^{RF} - S_n^{FF}$) was positive. This contrast in tactile perception is perhaps due to the viscoelastic properties of the fingertip and the hysteresis effect. [Wang and Hayward, 2007] have found that the skin deformed at a high rate when a step force was applied, but restored more slowly when the force was removed. In our experiments, the finger experienced lower tangential force followed by higher one under the condition of RF. Consequently, when we rendered RF, the finger deformed at a higher rate, which produced a stronger tactile feeling as compared to FF. Thus, the results of our experiments and literature suggest that the difference between RF and FF is due to viscoelasticity and not related to slower force transition in RF due to slower discharge of squeeze film [Meyer et al., 2014]. Viscoelastic materials show rate-dependent response and relaxation behavior. We argue that the increase in friction was more easily differentiated by subjects during RF due to the rate-dependent behavior compared to the friction drop during FF due to relaxation behavior. If viscoelasticity has an influence on our tactile perception, one anticipates that the experimental results of this study would be affected by finger velocity (f_v), which is not the case. The velocity range covered in our study (10-70 mm/s) is relatively small and the effect on tactile perception was not observable. The earlier studies in literature also show that the change in finger friction is observable only when there is a large difference in finger velocities [Adams et al., 2013]. The experiments performed by [Moy et al., 2000] indirectly support our claim. They asked the subjects to count the number of ridges scanned under their fingers. When a small ridge was presented before a big one, subjects perceived both ridges successfully. However, in opposite order, the subjects were not able to detect the small ridge. The authors argued that the poor perception of the small ridge after big one was due to the residual deformation of the fingertip due to hysteresis, as observed in viscoelastic materials.

Chapter 4

PERCEPTION OF CONSECUTIVE CHANGES IN FRICTION

To display realistic tactile textures on touch-enabled devices, it is important to understand how surface properties are perceived by means of touch in the real world. Earlier studies have shown that roughness is the most important dimension in tactile perception of textures [Okamoto et al., 2013, Hollins et al., 1993, Hollins et al., 2000, Bensmaïa and Hollins, 2005]. In this chapter, we are investigating the discrimination and roughness perception of virtual gratings rendered by ultrasonic actuation. First experiment investigates the spatial threshold to discriminate two consecutive changes in friction (called edges in the text), while the second experiment evaluates spatial discrimination of virtual periodic gratings rendered by a sequence of virtual edges. The roughness perception of virtual periodic gratings is finally investigated in third experimental study. To create an analogy between virtual and real gratings, we define the width of high friction regime (HFW) as a counterpart of ridge width (RW), and width of low friction regime (LFW) as a counterpart of groove width (GW), as shown in Figure 4.1. The schematic showing the hierarchy of the psychological experiments in this chapter is given in Figure 4.2.

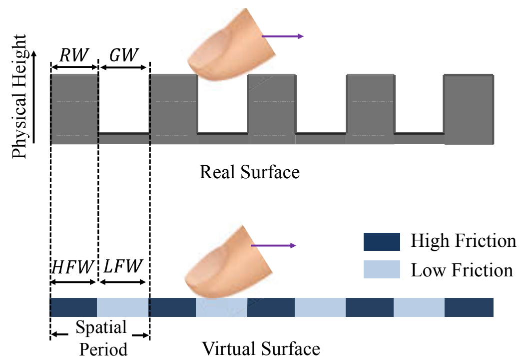

Figure 4.1: Analogy between real textures and virtual textures rendered in our study.

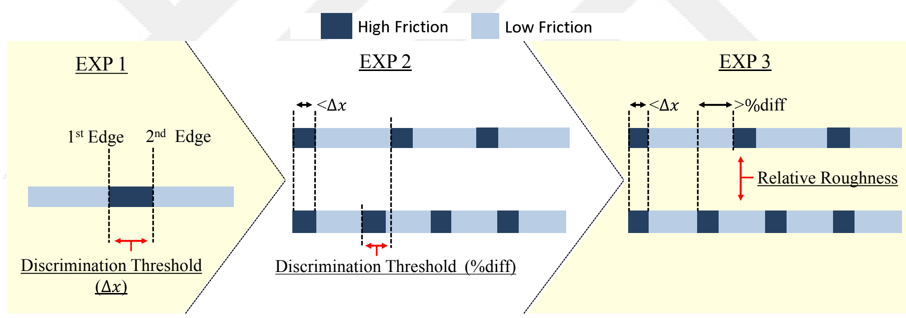

Figure 4.2: Hierarchy of experiments in this chapter.

4.1 EXP-1: Discrimination of Two Consecutive Virtual Edges

The purpose of this experiment was to estimate the spatial threshold between two consecutive virtual edges. An edge was rendered either by rising friction (RF) or falling friction (FF).

Twenty subjects (5 females) volunteered to take part in the experiment. The average age of the subjects was 28.8 ± 4.1 years. The subjects used the index finger of their dominant hand during the experiments. Their finger and the surface were cleaned with alcohol before the start of each experimental session. To eliminate any perceptual bias due to the surrounding noise, the subjects were asked to wear noise cancellation headphones, and white noise was played to their ears. There was a short training session at the start of each experiment to familiarize the subjects with the

Table 4.1: Rendering conditions for EXP-1. Note that the third column lists the desired values for V_{amp}, while the actual (measured) values are given in parenthesis.

Rendering Conditions	f_v (mm/s)	V_{amp} (µm)	E_{seq}
1	30	1 (0.91±0.07)	$FF \rightarrow RF$
2	30	1 (0.88±0.09)	$RF \rightarrow FF$
3	30	2 (1.80±0.16)	$FF \rightarrow RF$
4	30	2 (1.88±0.16)	$RF \rightarrow FF$
5	60	1 (0.88±0.07)	$FF \rightarrow RF$
6	60	1 (0.92±0.07)	$RF \rightarrow FF$
7	60	2 (1.80±0.13)	$FF \rightarrow RF$
8	60	2 (1.90±0.14)	$RF \rightarrow FF$

experimental setup and procedures. The subjects read and signed the consent form before the experiments. The form was approved by the Ethical Committee for Human Participants of Koc University.

4.1.1 Experimental Design

We considered three independent factors for the experimental design: finger velocity ($f_v = 30$ and 60 mm/s), vibration amplitude ($V_{amp} = 1$ and 2 µm), and edge sequence ($E_{seq} = FF \rightarrow RF$ and $RF \rightarrow FF$). In $FF \rightarrow RF$, we varied low friction width (LFW) between the two edges, while high friction width (HFW) was varied in $RF \rightarrow FF$ as elaborated in Figure 4.3(a). Therefore, there were a total of 8 rendering conditions as listed in Table 4.1.

4.1.2 Procedure

We rendered the first edge after moving subjects' finger via the motorized stage for 20 mm (to ensure steady motion), as shown in Figure 4.3(a). The distance (Δx) between two consecutive edges (i.e. LFW or HFW) was initially set to the maximum value of 15 mm but then adjusted dynamically based on the subjects' response. When

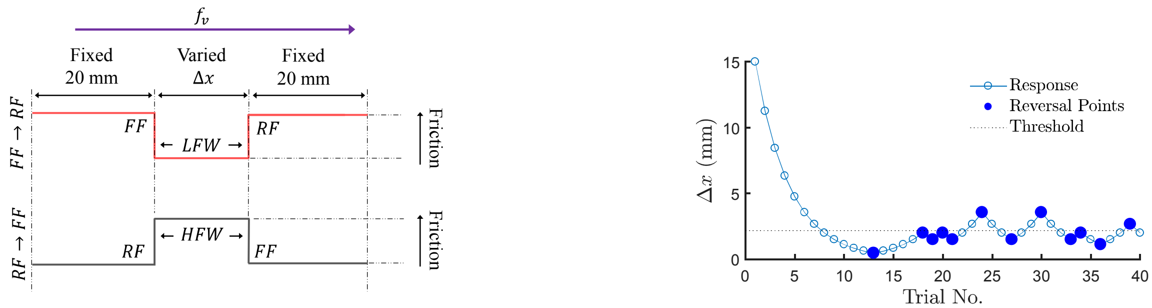

(a) (b)

Figure 4.3: Experimental procedure for evaluating the spatial threshold between two consecutive virtual edges (EXP-1). (a) Types of desired edge sequences (E_{seq}), (b) an example for experimental trial.

the motion was stopped, subjects were asked if they felt two distinct edges. If their response was "YES", we decreased Δx by 2.5 dB, however, if they reported only one edge ("NO" response), we increased Δx by 2.5 dB. We presented the stimuli on the rightward and leftward direction of their finger scan. The process was repeated for twelve reversals. If they could not detect two edges even after Δx of 15 mm, we restarted the experiment (twice only) after a short break. They were allowed to repeat any trial only once. They had to lift their finger up at the end of each scan to wait for the next one. We implemented this protocol to remove any build up stress on their finger during tangential motion. It took 5 to 7 minutes for subjects to reach a threshold value under each rendering condition. To reduce the learning effect, we permuted the order of rendering conditions by which subjects performed the experiment. Each subject completed the experiment in two days (four rendering conditions per day).

We calculated the spatial threshold (Δx) by averaging the last eight reversals of each trial (see Figure 4.3(b)). The spatial threshold values were converted to temporal ones using $\Delta t = \Delta x / f_v$. We performed three-way repeated measure ANOVA to analyze the effects of independent factors f_v, V_{amp}, and E_{seq} on spatial threshold. For pair-wise comparisons, the significance level for each comparison was adjusted using Bonferroni correction.

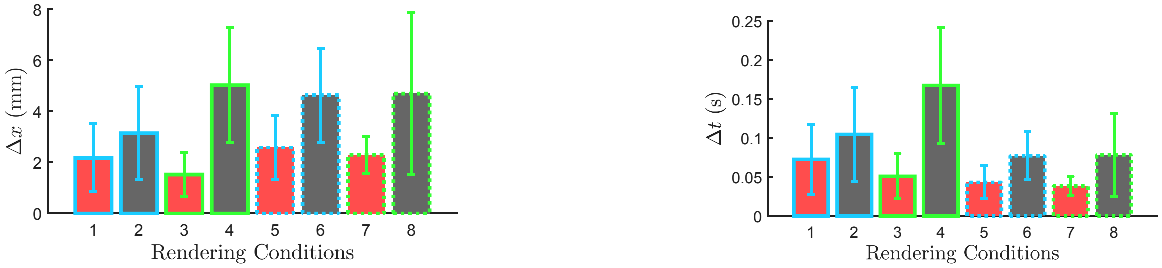

(a) (b)

Figure 4.4: Thresholds to discriminate two consecutive virtual edges in EXP-1 (mean values and standard deviations); a) spatial threshold, and b) temporal threshold. Red and gray bars are for $FF \rightarrow RF$ and $RF \rightarrow FF$, solid and dotted bars are for f_v of 30 and 60 mm/s, blue and green bars are for V_{amp} of 1 and 2 µm, respectively.

4.1.3 Results

During the experiment, some subjects had difficulty in detecting two consecutive edges under the condition of $RF \rightarrow FF$. A few amongst them reported that they could feel a sharp rise in friction followed by a slower decrease, which they could not classify as an edge. However, almost all subjects performed very well under $FF \rightarrow RF$. For further analysis, we only considered the results of 12 subjects (5 females) who showed converging response under all rendering conditions. The discrimination thresholds in spatial and temporal domains (Δx and Δt) for all rendering conditions are shown in Figure 4.4(a) and Figure 4.4(b), respectively. The mean thresholds against all independent factors are listed in Table 4.2.

- The results showed that the effect of finger velocity (f_v) on spatial threshold was not significant ($F(1, 11) = 3.0, p = 0.11$).
- The spatial threshold was significantly lower for $FF \rightarrow RF$, as compared with $RF \rightarrow FF$ ($F(1, 11) = 25.9, p < 0.001$).
- There was no significant effect of vibration amplitude (V_{amp}) on spatial threshold. However, we observed an interaction effect of $V_{amp} \times E_{seq}$ on the spatial threshold ($F(1, 11) = 12.7, p = 0.004$). A post-hoc analysis showed that V_{amp}

Table 4.2: Mean thresholds to discriminate two consecutive virtual edges (EXP-1).

Independent Factors		$\Delta x \pm$ SEM (mm)	$\Delta t \pm$ SEM (s)
f_v	30 mm/s	2.94±0.35	0.10±0.01*
	60 mm/s	3.60±0.42	0.06±0.01*
V_{amp}	1 µm	3.11±0.33	0.07±0.01
	2 µm	3.40±0.42	0.08±0.01
E_{seq}	$FF \rightarrow RF$	2.14±0.26*	0.05±0.01*
	$RF \rightarrow FF$	4.45±0.57*	0.11±0.01*

*Statistically significant

affected $RF \rightarrow FF$ ($p = 0.05$). This is evident if rendering conditions 2 and 4 are compared in Figure 4.4(a).

4.2 EXP-2: Discrimination of Virtual Periodic Gratings

The goal of the second experiment was to estimate the difference threshold between spatial periods of two periodic gratings.

Eleven subjects (4 females) with an average age of 30.2 ± 2.9 years participated in the experiment. The experimental and ethical protocols followed in this experiment were the same as in EXP-1 in this chapter.

4.2.1 Experimental Design

We considered three independent factors; rendering length (R_{length} = 20, 30, and 40 mm), finger velocity (f_v = 30 and 60 mm/s), and waveform ($W_{frm} = W^1_{frm}$ and W^2_{frm}). The vibration amplitude (V_{amp}) was fixed to 1 µm. Therefore, there were a total of 12 rendering conditions (see Table 4.3). In W^1_{frm}, we fixed low friction width (LFW) and varied high friction width (HFW), while in W^2_{frm}, we fixed HFW and varied LFW (Figure 4.5(a)). The fixed width in both waveforms was taken as 1 mm, which was below the spatial threshold estimated in EXP-1. This ensured that two edges across fixed width were perceived as a single pulse by the subjects. Therefore,

Table 4.3: Rendering conditions for EXP-2.

Rendering Conditions	R_{length} (mm)	f_v (mm/s)	W_{frm}
1	20	30	1
2	20	30	2
3	20	60	1
4	20	60	2
5	30	30	1
6	30	30	2
7	30	60	1
8	30	60	2
9	40	30	1
10	40	30	2
11	40	60	1
12	40	60	2

in W^1_{frm}, we rendered a multiple sequence of consecutive edges $FF \rightarrow RF$ (i.e. a series of pulses resulting in high friction between fingerpad and the touch surface on average). In W^2_{frm}, we rendered a multiple sequence of $RF \rightarrow FF$ (i.e. a series of pulses resulting in low friction between fingerpad and the touch surface on average), as depicted in Figure 4.5(a).

4.2.2 Procedure

We rendered gratings with higher and lower number of friction pulses on the alternative directions (rightward and leftward) of finger scan. At the start of the experiment, we rendered one vs. two pulses on the alternative directions but then monotonically increased/decreased the number of pulses by two in each direction based on subjects' response while keeping the difference as one always. The direction in which we rendered a higher number of pulses was randomized during each trial. Subjects had to identify the direction (rightward or leftward) in which they felt more number of friction pulses. We used three up and one down transformed staircase method as

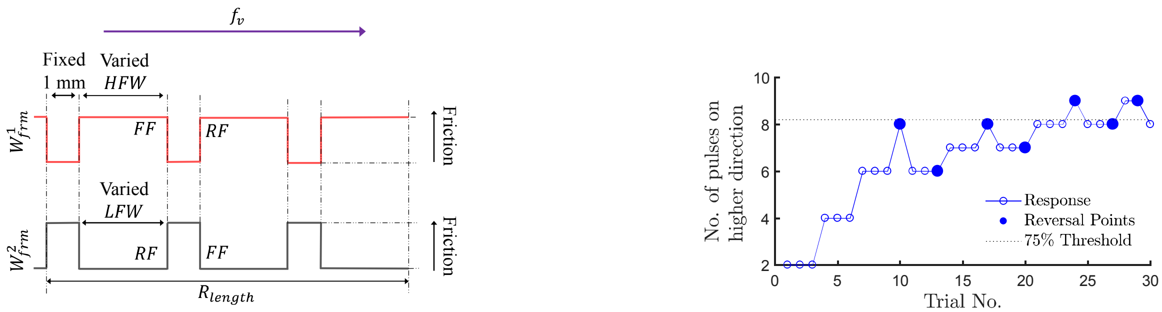

(a) (b)

Figure 4.5: Experimental procedure for evaluating the difference threshold between spatial periods of two virtual textures in EXP-2. (a) Types of desired waveforms (W_{frm}), (b) an example for experimental trial.

elaborated in [Zwislocki and Relkin, 2001], which converges on the 75% correct level. Hence, if subjects gave three correct answers, we increased the number of pulses in alternative directions to three vs. four, five vs. six, seven vs. eight, and so on. In case of a wrong answer, we decreased the number of pulses by two in each direction. The step size was reduced to one pulses after the first reversal. The experiment was stopped after seven reversals. Similar to EXP-1, subjects were allowed to repeat any trial only once, and we permuted the order of rendering conditions by which subjects performed the experiment. Each subject completed the experiment in three days (four rendering conditions per day).

We estimated the convergent value for lower and higher number of pulses by averaging the last five reversals as shown in Figure 4.5(b), and then rounded it to the nearest integer. Then, we calculated the spatial periods SP^{high} and SP^{low} corresponding to the lower and higher number of pulses, respectively. To interpret the results, we calculated the absolute difference between spatial periods ($\Delta SP= SP^{high} - SP^{low}$), mean spatial period ($\overline{SP}= (SP^{high} + SP^{low})/2$), and the relative difference between spatial periods (R_{diff}=$\Delta SP/\overline{SP}\times 100$) at the threshold level. We performed three-way repeated measure ANOVA to analyze the effects of independent factors R_{length}, f_v and, W_{frm} on R_{diff}. During the statistical analysis, we adjusted the degree of freedom using Greenhouse-Geisser correction whenever the sphericity assumption was

Table 4.4: Mean thresholds to discriminate virtual periodic gratings (EXP-2).

Independent Factors		$\Delta SP \pm$ SEM (mm)	$\overline{SP} \pm$ SEM (mm)	$R_{diff} \pm$ SEM (%)
R_{length}	20 mm	0.44±0.05*	2.9±0.16*	14.2±0.8
	30 mm	0.73±0.10*	4.4±0.32*	14.7±1.1
	40 mm	0.84±0.09*	5.6±0.32*	14.0±0.8
f_v	30 mm/s	0.58±0.07*	4.0±0.26*	13.3±0.8*
	60 mm/s	0.76±0.08*	4.6±0.26*	15.3±0.9*
W_{frm}	1	0.64±0.07	4.2±0.23	14.0±0.7
	2	0.71±0.09	4.4±0.28	14.7±0.9

*Statistically significant

violated.

4.2.3 Results

The mean thresholds for all independent factors are tabulated in Table 4.4. The results showed that:

- Increasing the rendering length (R_{length}), also increased the absolute difference between spatial period, ΔSP ($F(2, 20) = 12.5, p < 0.001$) and mean spatial period, $\overline{SP}$ ($F(2, 20) = 52.9, p < 0.001$) required to differentiate two virtual gratings. However, the relative difference between spatial periods (R_{diff}) remained the same with no significant effect of R_{length} ($F(2, 30) = 0.37, p = 0.69$), as shown in Fig 4.6.

- R_{diff} slightly increased with increasing finger velocity, f_v ($F(1, 10) = 6.25, p = 0.031$).

- ANOVA test reviled no significant effect of waveform (W_{frm}) on R_{diff} ($F(1, 10) = 1.03, p = 0.33$), and no significant interaction between the independent factors.

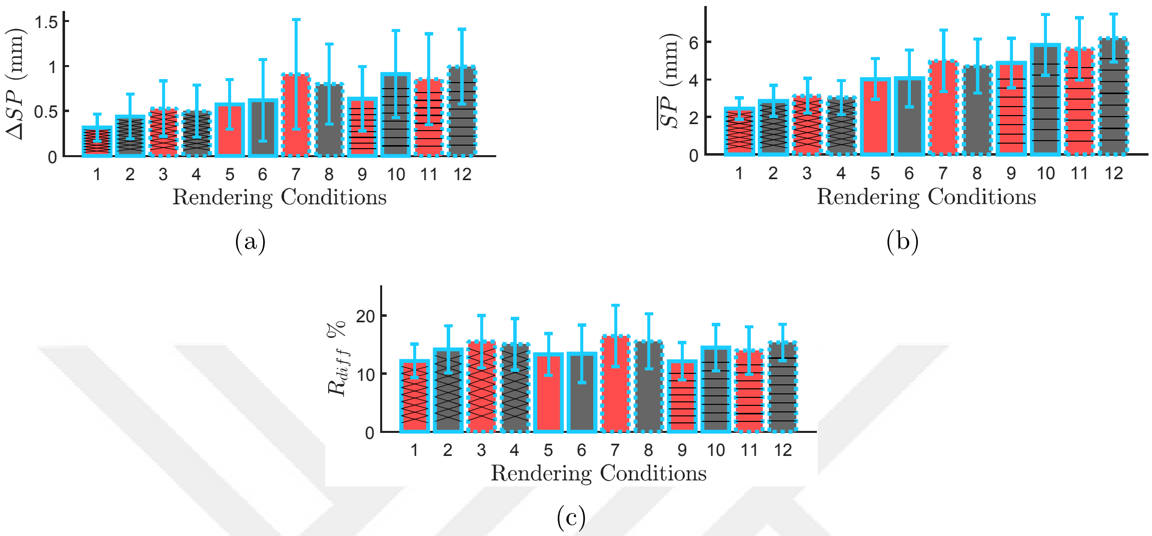

Figure 4.6: Thresholds to discriminate virtual periodic textures in EXP-2 (mean values and standard deviations); a) absolute difference between spatial periods, b) mean spatial periods, and c) relative difference between spatial periods. Red and gray bars are for W^1_{frm} and W^2_{frm}, solid and dotted bars are for f_v of 30 and 60 mm/s, respectively. Cross, plain and horizontal hatched bars are for R_{length} of 20, 30 and 40 mm, respectively.

4.3 EXP-3: Roughness Perception of Virtual Gratings

We investigated the roughness perception of virtual textures in spatial and temporal domains.

Eleven subjects (3 females) with an average age of 29.7 ± 3.9 years participated in this experiment. The experimental and ethical protocols followed in this experiment were the same as in EXP-1.

4.3.1 Experimental Design

To investigate the roughness perception, we selected three independent factors: spatial period (SP), finger velocity ($f_v = 30$ and 60 mm/s), and waveform ($W_{frm} = W^1_{frm}$ and W^2_{frm}). We have chosen seven different SPs in macro-texture range, varying from 2.5 to 7.4 mm with an increment of 20% as shown in Figure 4.7. The increment (20%) was selected as higher than the relative threshold value estimated in EXP-2.

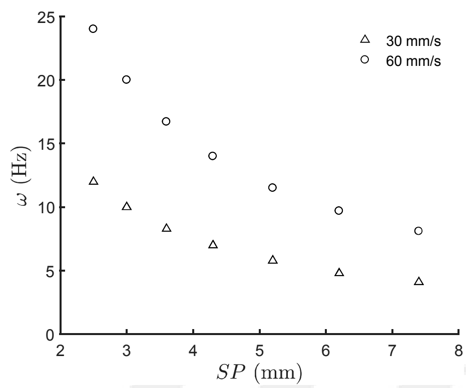

Figure 4.7: Spatial period (SP) and temporal frequency (ω=SP/f_v) of virtual textures rendered in roughness perception experiment (EXP-3).

We fixed rendering length (R_{length}) to 30 mm, and vibration amplitude (V_{amp}) to 1 µm in this experiment. Hence, there were 28 rendering conditions, repeated 10 times, making a total of 280 trials for each subject.

4.3.2 Procedure

We rendered each stimulus on the rightward scan first. Then, subjects lifted their finger up and the same stimulus was repeated on the leftward scan. We monitored the mean normal force ($\overline{F_n}$) on both scans. If $\overline{F_n}$ was outside the desired range (0.25 ± 15% N), the subjects were prompted to repeat the trial. We have chosen $\overline{F_n}$ of 0.25 N because this was the most comfortable force reported by a number of subjects during the preliminary experiments. On the completion of each trial, the subjects were asked to rate the roughness they perceived using an integer value with no constraints on its limit (a higher number for rougher surface). They were allowed to repeat each stimulus twice only. The trials were randomized, while the same randomization pattern was used for each subject. The experiment took approximately 45 minutes, and subjects completed it in two sessions.

For the analysis, we first normalized the roughness estimates of each subject. For that, we divided the scores of each subject by his/her geometric mean, and then multiplied it with the overall geometric mean of all subjects. We performed three-way

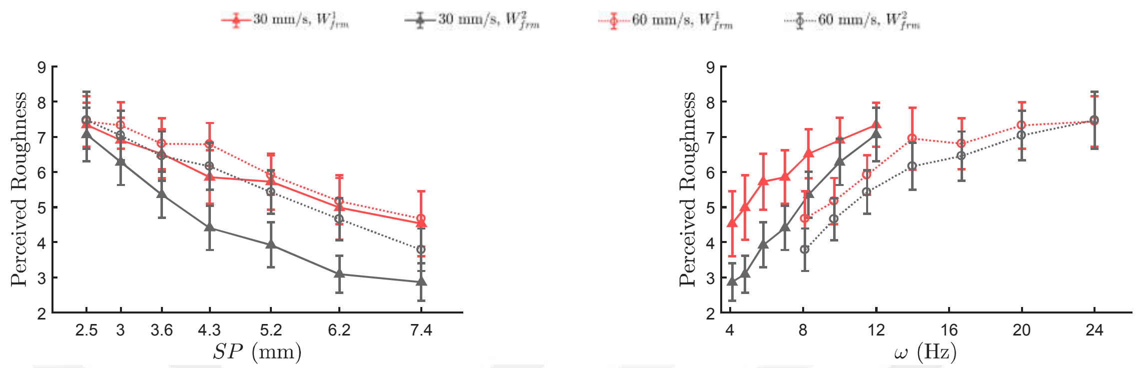

(a) (b)

Figure 4.8: Perceived roughness (mean values and standard errors) of virtual textures in spatial (a) and temporal (b) domains.

repeated measure ANOVA to analyze the effects of f_v, W_{frm} and SP on normalized roughness score. We adjusted the degree of freedom using Greenhouse-Geisser correction whenever necessary. For pair-wise comparisons, the significance level was adjusted by Bonferroni correction.

We also analyzed the force data recorded during the experiment to calculate metrics based on friction coefficient. To calculate friction coefficient ($\mu = F_t/F_n$), we took a window of duration $t^{total} = R_{length}/f_v$, starting from the moment we rendered the first edge. The mean value of friction coefficient ($\overline{\mu}$) was calculated by averaging μ for the interval of t^{total}. To analyze the rate of change in friction ($d\mu/dt$), we computed its RMS value for each spatial period, and then calculated the overall average for all spatial periods ($\overline{d\mu/dt}$). Finally, we used Spearman correlation to investigate the relation between roughness perception and friction metrics.

4.3.3 Results

The mean roughness scores of subjects in spatial and temporal domains are reported in Figure 4.8(a) and Figure 4.8(b), respectively. The results showed that:

- Perceived roughness decreased with spatial period, SP ($F(1.1, 11.3) = 23.1, p < 0.001$), and increased with finger velocity, f_v ($F(1, 10) = 6.91, p = 0.025$).

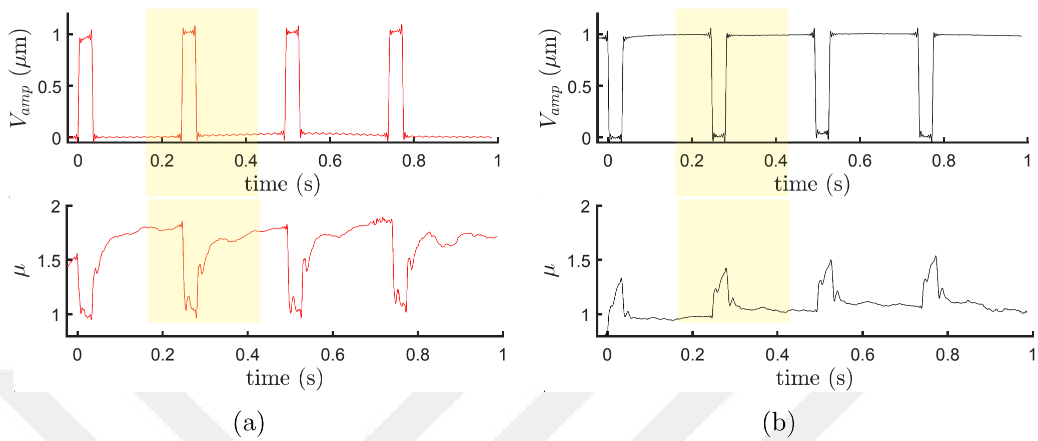

Figure 4.9: Vibration amplitude and friction coefficient recorded at 30 mm/s for a) W^1_{frm} and b) W^2_{frm}.

- The subjects perceived W^1_{frm} significantly rougher than W^2_{frm} ($F(1, 10) = 8.90, p = 0.014$).
- There was a significant interaction effect of $SP \times f_v$ ($F(6, 60) = 6.8, p < 0.001$), and $SP \times W_{frm}$ ($F(6, 60) = 5.8, p < 0.001$) on perceived roughness. Post-hoc pairwise analysis showed that effect of W_{frm} was significant for $SP \geq 3$ mm ($p = 0.04$), and effect of f_v was significant for $SP \geq 4.6$ mm ($p = 0.001$).
- The modulated friction profile resembled to desired square signal more for W^1_{frm} as than W^2_{frm} (Figure 4.9).
- There was a significant effect of W_{frm} and SP ($p < 0.001$) on $\overline{\mu}$ and $\overline{d\mu/dt}$ (Figure 4.10).
- There was a significant effect of f_v on $\overline{d\mu/dt}$ ($p = 0.05$).
- Correlation analysis between roughness scores and friction metrics showed a moderate correlation for $\overline{d\mu/dt}$ ($r_s = 0.58, n = 308, p < 0.001$) and a weak correlation for $\overline{\mu}$ ($r_s = 0.30, n = 308, p < 0.001$).

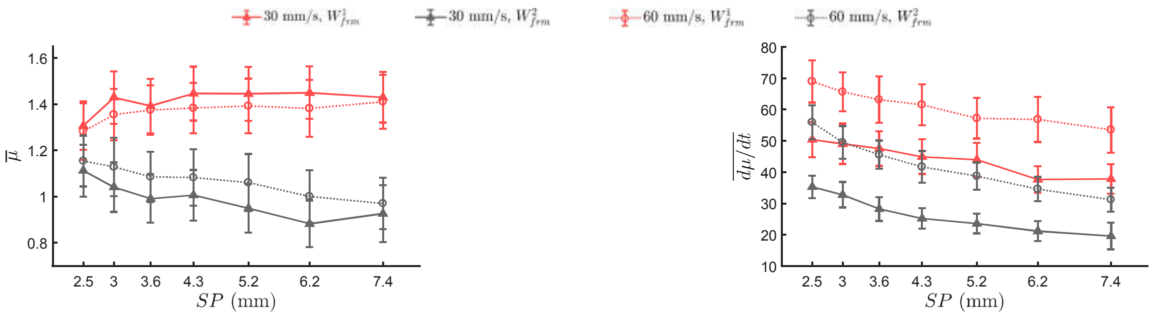

(a) (b)

Figure 4.10: Friction metrics (mean values and standard errors).

4.4 Discussion

4.4.1 Discrimination Threshold for Two Virtual Edges

In EXP-1, we measured the spatial threshold distance (Δx) between two consecutive edges under $FF \to RF$ as 2 mm. Interestingly, this value is approximately equal to the two-point discrimination resolution of human index finger [Won et al., 2017]. Tactile perception of virtual edges rendered by ultrasonic actuation was also investigated by [Gueorguiev et al., 2017b] in temporal domain. However, they did not control finger velocity, while vibration amplitude was actively maintained at 1.25 µm. They reported a temporal threshold duration of 0.05 s. Hence, our results supported their observation, as we also found temporal threshold duration (Δt) of 0.05 s under $FF \to RF$. In case of $RF \to FF$, the threshold value was higher, indicating that it was more difficult for the subjects to discriminate two edges under this condition. As shown in Figure 4.9 (see the shaded window), $FF \to RF$ produced a sharper change in friction response as compared with $RF \to FF$. This was due to the slower dynamics of rising friction (RF) than falling friction (FF), which is in line with earlier findings [Meyer et al., 2014]. Hence, it is not surprising that subjects detected two consecutive edges more easily under $FF \to RF$.

4.4.2 Discrimination of Virtual Periodic Gratings

The results of EXP-2 showed that a relative difference (R_{diff}) of 14% in spatial period was necessary to differentiate virtual periodic gratings. [Biet et al., 2008a] have reported a Weber fraction of 9% for the discrimination of two periodic square gratings, rendered by ultrasonic actuation. Several factors might have contributed to the difference; we used a staircase method, and the two gratings being compared in our study were always differed by one spatial period only, which makes it more difficult to differentiate them. On the other hand, spatial period was altered explicitly using the method of constant stimuli in [Biet et al., 2008a]. Furthermore, we controlled the finger velocity (f_v), and the subjects were allowed to explore a stimulus only twice. However, finger velocity was not controlled, and there was no limit on exploration time in [Biet et al., 2008a]. Nevertheless, the spatial discrimination thresholds of virtual square gratings tested in our study and [Biet et al., 2008a] are higher than the real ones [Morley et al., 1983].

4.4.3 Roughness Perception of Virtual Gratings

The results of EXP-3 showed that perceived roughness decreased with increasing spatial period (SP), though the decrease was more significant for W^2_{frm}, as expected (Figure 4.10(a)). A similar decrease in roughness perception with increasing spatial period has been reported for virtual textures rendered by electrovibration [Vardar et al., 2017b], and also for a force feedback device that can display tangential forces only [Smith et al., 2010]. On the other hand, roughness perception of real periodic textures increases with increasing groove width, but decreases slightly with increasing ridge width [Taylor and Lederman, 1975, Lederman, 1983, Morley et al., 1983, Sathian et al., 1989, Yoshioka et al., 2001, Cascio and Sathian, 2001, Lawrence et al., 2007, Drewing, 2018]. Nevertheless, a decrease in roughness perception with increasing spatial period was observed for linear gratings when the height of ridges was low [Drewing, 2016]. Therefore, the difference in perception between the real textures in the earlier studies and the virtual textures in studies [Smith et al., 2010, Vardar et al., 2017b] and also our study is not surprising due to missing spatial cues on height in virtual textures rendered by friction modulation. Correlation analysis showed a moderate positive correlation between perceived roughness and rate of change in friction coefficient ($\overline{d\mu/dt}$), as also reported earlier by others for real [Smith et al., 2002] and virtual [Vardar et al., 2017b] periodic gratings. On the other hand, a significant correlation between friction coefficient and roughness perception was reported in [Smith et al., 2010], though we observed a weak correlation. As shown in Figure 4.10, W^1_{frm} resulted in higher $\overline{\mu}$ and $\overline{d\mu/dt}$ on average as compared with W^2_{frm}. This explains why W^1_{frm} was perceived rougher than W^2_{frm} (Figure 4.8).

The results of our experiment also showed that, despite doubling of finger velocity (f_v), the maximum perceived roughness remained almost the same (see roughness scores for $SP = 2.5$ mm rendered at $\omega = 12$ and 24 Hz in Figure 4.8(b)). Therefore, the results rejected our initial hypothesis that the perception of virtual periodic textures is more dominantly governed by temporal cues since spatial cues in normal direction cannot be rendered directly by friction modulation. In fact, effect of spatial cues on roughness perception of virtual textures raises several questions regarding the underlying neural mechanism. The maximum value of ω in our experiments was significantly lower than the sensitivity range (80 Hz and above, [Freeman and Johnson, 1982]) of PC afferents. Yet, [Vardar et al., 2017a] showed that PC afferents play an important role in the detection of square gratings rendered by electrovibration at low frequencies (< 60 Hz). However, if the decrease in roughness perception was primarily mediated by PC afferents, then one should expect a dominant effect of temporal frequency, as observed in [Cascio and Sathian, 2001], which was not the case in our experiment. Similarly, it is less likely that SA1 afferents have played a significant role in the tactile perception of virtual textures in our experiment due to missing spatial cues on texture height. Although, SA1 afferents are also sensitive to tactile slip due to skin deformation [Srinivasan et al., 1990], the performance degrades rapidly above 5 Hz [Freeman and Johnson, 1982]. On the other hand, RA-afferents respond more robustly to coarser textures [Johnson, 2001, Weber et al., 2013] and four times

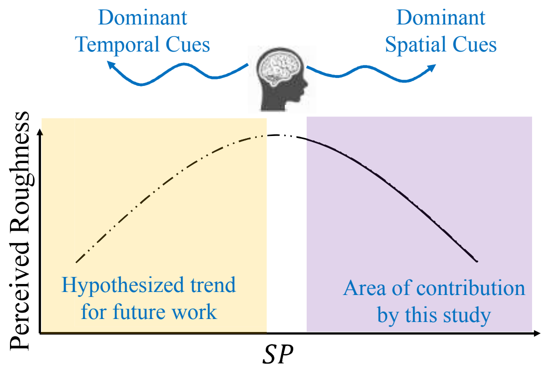

Figure 4.11: A hypothetical curve explaining the roughness perception of virtual textures.

more sensitive to dynamic skin deformation than SA1 afferents, and provide essential feedback for grip control through micro-slips. They respond to low frequency stimuli more robustly than PC afferents [Freeman and Johnson, 1982, Johnson et al., 2000, Johnson, 2001]. Using microneurography technique, [Birznieks et al., 2001] showed that SAI, SAII and RA afferents all respond to tangential forces applied to the human fingerpad. They observed that RA afferents respond more strongly for tangential forces in radial direction, while SA1 and SA2 afferents are biased towards distal and proximal directions, respectively. Therefore, RA afferents might have played a role in the perception of virtual textures rendered in our study. Furthermore, [Moscatelli et al., 2014] have shown that humans can estimate the length of spatial paths from the tactile slips displayed on the fingerpad using a servo controlled rotating ball. Hence, it is quite possible that our subjects were able to resolve successive micro-slips to spatial periods with the help of RA afferents. However, further investigation is indeed required to better understand the underlying neural mechanism.

On the other hand, we should point out that effect of spatial cues on roughness perception is likely to be valid within our tested range of spatial periods only. A trend of flattening or decrease in roughness perception at smaller spatial periods (i.e higher temporal frequency) is reported for virtual textures in [Vardar et al., 2017b, Unger et al., 2011]. Similarly, [Ahmaniemi et al., 2010] investigated the perception of virtual textures displayed by a hand held vibrotactile actuator. They reported that the textures created with a carrier frequency of 10 Hz were perceived rougher than those of 20 Hz. Therefore, an inverted U-shaped trend is likely to be observed when micro textures are investigated, which is the topic of our future studies (Figure 4.11).

Chapter 5

CONCLUSION AND FUTURE WORK

Using an ultrasonic tactile display, we investigated our tactile perception of change in friction (virtual edge), rendered by rising friction (RF) and falling friction (FF). For a sliding-finger, subjects' psychometric curves for RF and FF were almost identical, while they felt the friction change for FF only when they gently pressed their finger on the surface without sliding, as in key press. On the other hand, when the sliding experiment was repeated at stimuli levels significantly higher than the detection threshold level, RF was perceived more strongly than FF. These results suggest that the factors affecting our tactile perception of friction change for sliding are different than those of no-sliding. For sliding-finger, our results suggest that the perceived intensity of friction change was best correlated with tangential force contrast (F_tC) and rate of change in tangential force (dF_t/dt). A simple linear model using only those two metrics estimated the subjects' perception quite well. However, the difference between the correlation coefficients for F_tC and μC was not significant, as tabulated in Table 3.5. Either can be used with dF_t/dt to estimate the subjects' perception.

Intensity scaling experiments showed that the finger velocity has little or almost no effect on our tactile perception of virtual edges. However, subjects' perception was affected by the transition time (i.e. slope of the friction change) and the normal force. As the transition time was longer (and hence the slope was lower), the strength of their perception was reduced. As the normal force was increased, subjects perceived a stronger change in friction, though the perceptual difference between RF and FF was reduced. However, the effects of finger velocity, transition time and normal force on threshold levels cannot be ascertained by our experiments.

We proposed that the perceptual difference between RF and FF during finger sliding was due to viscoelastic properties of fingertip. We supported this claim by relating our results with those of the earlier studies in the literature. In order to provide a further support, skin deformations in fingertip can be analyzed during friction change, using a high-speed camera and computer vision techniques, as done in [Wiertlewski et al., 2016].

In this second part of the thesis, we investigated the spatial discrimination of virtual edges and roughness perception of virtual square gratings generated by consecutive virtual edges, all in macro-scale. We observed that virtual edges were detected by the subjects if the distance between them (spatial threshold) was more than 2 mm, provided that the first edge was rendered by a FF and second one by a RF. In the case of opposite edge sequence, the mean distance between the edges was above 4 mm. We found that a relative difference of 14% in spatial period is necessary in perceived roughness for the discrimination of virtual gratings. Finally, we investigated the roughness perception of virtual gratings for different spatial periods. The results showed that the roughness perception of square gratings followed a decreasing trend with increasing spatial period, and rate of change in friction was more strongly correlated with roughness perception than friction coefficient itself. The results also suggested spatial period played a significant role in roughness perception of virtual gratings rendered by ultrasonic actuation despite the missing spatial cues in the direction normal to the touch surface.

Our results are valid for macro-textures having a spatial period greater than 2 mm. The open-loop nature of our system prevented us from studying finer textures. Future work involves investigating the roughness perception of virtual textures over a wider range (see Fig. 4.11). Furthermore, possible effect of vibrotactile masking on tactile discrimination and roughness perception is another avenue that we would like to explore. We hope that this will shed further light on the mechanisms behind our perception of friction and change in friction rendered on touch surfaces.

BIBLIOGRAPHY

[Adams et al., 2007] Adams, M. J., Briscoe, B. J., and Johnson, S. A. (2007). Friction and lubrication of human skin. *Tribology Letters*, 26(3):239–253.

[Adams et al., 2013] Adams, M. J., Johnson, S. A., Lefèvre, P., Lévesque, V., Hayward, V., André, T., and Thonnard, J.-L. (2013). Finger pad friction and its role in grip and touch. *Journal of The Royal Society Interface*, 10(80).

[Ahmaniemi et al., 2010] Ahmaniemi, T., Marila, J., and Lantz, V. (2010). Design of dynamic vibrotactile textures. *IEEE Transactions on Haptics*, 3(4):245–256.

[André et al., 2009] André, T., Lefvre, P., and Thonnard, J.-L. (2009). A continuous measure of fingertip friction during precision grip. *Journal of Neuroscience Methods*, 179(2):224 – 229.

[Bau et al., 2010] Bau, O., Poupyrev, I., Israr, A., and Harrison, C. (2010). Teslatouch: Electrovibration for touch surfaces. In *Proceedings of the 23rd Annual ACM Symposium on User Interface Software and Technology*, UIST '10, pages 283–292, New York, NY, USA. ACM.

[Ben Messaoud et al., 2016] Ben Messaoud, W., Bueno, M.-A., and Lemaire-Semail, B. (2016). Textile fabrics' texture: From multi-level feature extraction to tactile simulation. In Bello, F., Kajimoto, H., and Visell, Y., editors, *Haptics: Perception, Devices, Control, and Applications*, pages 294–303, Cham. Springer International Publishing.

[Bensmaïa and Hollins, 2005] Bensmaïa, S. and Hollins, M. (2005). Pacinian representations of fine surface texture. *Perception & Psychophysics*, 67(5):842–854.

[Bernard et al., 2018] Bernard, C., Monnoyer, J., and Wiertlewski, M. (2018). Harmonious textures: The perceptual dimensions of synthetic sinusoidal gratings. In Prattichizzo, D., Shinoda, H., Tan, H. Z., Ruffaldi, E., and Frisoli, A., editors, *Haptics: Science, Technology, and Applications*, pages 685–695, Cham. Springer International Publishing.

[Biet et al., 2008a] Biet, M., Casiez, G., Giraud, F., and Lemaire-Semail, B. (2008a). Discrimination of virtual square gratings by dynamic touch on friction based tactile displays. In *Symposium on Haptic Interfaces for Virtual Environment and Teleoperator Systems*, pages 41–48.

[Biet et al., 2008b] Biet, M., Giraud, F., and Lemaire-Semail, B. (2008b). Implementation of tactile feedback by modifying the perceived friction. *Eur. Phys. J. Appl. Phys.*, 43(1):123–135.

[Birznieks et al., 2001] Birznieks, I., Jenmalm, P., Goodwin, A. W., and Johansson, R. S. (2001). Encoding of direction of fingertip forces by human tactile afferents. *Journal of Neuroscience*, 21 20:8222–8237.

[Blake et al., 1997] Blake, D. T., Hsiao, S. S., and Johnson, K. O. (1997). Neural coding mechanisms in tactile pattern recognition: The relative contributions of slowly and rapidly adapting mechanoreceptors to perceived roughness. *Journal of Neuroscience*, 17(19):7480–7489.

[Cascio and Sathian, 2001] Cascio, C. J. and Sathian, K. (2001). Temporal cues contribute to tactile perception of roughness. *Journal of Neuroscience*, 21(14):5289–5296.

[Chen et al., 2009] Chen, X., Shao, F., Barnes, C., Childs, T., and Henson, B. (2009). Exploring relationships between touch perception and surface physical properties. *International Journal of Design*, 3(2):67–76.

[Connor et al., 1990] Connor, C., Hsiao, S., Phillips, J., and Johnson, K. (1990). Tactile roughness: Neural codes that account for psychophysical magnitude estimates. *Journal of Neuroscience*, 10(12):3823–3836.

[Connor and Johnson, 1992] Connor, C. and Johnson, K. (1992). Neural coding of tactile texture: comparison of spatial and temporal mechanisms for roughness perception. *Journal of Neuroscience*, 12(9):3414–3426.

[Cornuault et al., 2015] Cornuault, P.-H., Carpentier, L., Bueno, M.-A., Cote, J.-M., and Monteil, G. (2015). Influence of physico-chemical, mechanical and morphological fingerpad properties on the frictional distinction of sticky/slippery surfaces. *Journal of The Royal Society Interface*, 12(110).

[Dai et al., 2012] Dai, X., Colgate, J. E., and Peshkin, M. A. (2012). Lateralpad: A surface-haptic device that produces lateral forces on a bare finger. In *2012 IEEE Haptics Symposium (HAPTICS)*, pages 7–14.

[Delhaye et al., 2016] Delhaye, B., Barrea, A., Edin, B. B., Lefèvre, P., and Thonnard, J.-L. (2016). Surface strain measurements of fingertip skin under shearing. *Journal of The Royal Society Interface*, 13(115).

[Delhaye et al., 2014] Delhaye, B., Lefèvre, P., and Thonnard, J.-L. (2014). Dynamics of fingertip contact during the onset of tangential slip. *Journal of The Royal Society Interface*, 11(100).

[Derler et al., 2009] Derler, S., Gerhardt, L.-C., Lenz, A., Bertaux, E., and Hadad, M. (2009). Friction of human skin against smooth and rough glass as a function of the contact pressure. *Tribology International*, 42(11):1565 – 1574.

[Drewing, 2016] Drewing, K. (2016). Low-amplitude textures explored with the bare finger: Roughness judgments follow an inverted U-shaped function of texture period modified by texture type. In Bello, F., Kajimoto, H., and Visell, Y., editors, *Haptics: Perception, Devices, Control, and Applications*, pages 206–217, Cham. Springer International Publishing.

[Drewing, 2018] Drewing, K. (2018). Judged roughness as a function of groove frequency and groove width in 3D-printed gratings. In Prattichizzo, D., Shinoda, H., Tan, H. Z., Ruffaldi, E., and Frisoli, A., editors, *Haptics: Science, Technology, and Applications*, pages 258–269, Cham. Springer International Publishing.

[Drewing et al., 2004] Drewing, K., Ernst, M. O., Lederman, S. J., and Klatzky, R. (2004). Roughness and spatial density judgments on visual and haptic textures using virtual reality. *Proceeding of the 4th International Conference Euro-Haptics*, pages 203–206.

[Emgin et al., 2018] Emgin, S. E., Aghakhani, A., Sezgin, M., and Basdogan, C. (2018). Haptable: An interactive tabletop providing online haptic feedback for touch gestures. *IEEE Transactions on Visualization and Computer Graphics*, pages 1–1.

[Fagiani et al., 2012] Fagiani, R., Massi, F., Chatelet, E., Costes, J. P., and Berthier, Y. (2012). Contact of a finger on rigid surfaces and textiles: Friction coefficient and induced vibrations. *Tribology Letters*, 48(2):145–158.

[Freeman and Johnson, 1982] Freeman, A. W. and Johnson, K. O. (1982). A model accounting for effects of vibratory amplitude on responses of cutaneous mechanoreceptors in macaque monkey. *The Journal of Physiology*, 323(1):43–64.

[Friesen et al., 2018] Friesen, R. F., Klatzky, R. L., Peshkin, M. A., and Colgate, J. E. (2018). Single pitch perception of multi-frequency textures. In *IEEE Haptics Symposium (HAPTICS)*, pages 290–295.

[Giraud et al., 2013] Giraud, F., Amberg, M., and Lemaire-Semail, B. (2013). Design and control of a haptic knob. *Sensors and Actuators A: Physical*, 196:78 – 85.

[Gueorguiev, 2016] Gueorguiev, D. (2016). *" Tactile perception of natural and simulated textures: a psychophysical approach*. PhD thesis, Université catholique de Louvain.

[Gueorguiev et al., 2016] Gueorguiev, D., Bochereau, S., Mouraux, A., Hayward, V., and Thonnard, J.-L. (2016). Touch uses frictional cues to discriminate flat materials. *Scientific Reports*, 6.

[Gueorguiev et al., 2017a] Gueorguiev, D., Vezzoli, E., Mouraux, A., Lemaire-Semail, B., and Thonnard, J.-L. (2017a). The tactile perception of transient changes in friction. *Journal of The Royal Society Interface*, 14(137).

[Gueorguiev et al., 2017b] Gueorguiev, D., Vezzoli, E., Sednaoui, T., Grisoni, L., and Lemaire-Semail, B. (2017b). Feeling multiple edges: The tactile perception of short ultrasonic square reductions of the finger-surface friction. In *IEEE World Haptics Conference (WHC)*, pages 125–129.

[Guzererler et al., 2016] Guzererler, A., Provancher, W. R., and Basdogan, C. (2016). Perception of skin stretch applied to palm: Effects of speed and displacement. In *Haptics: Perception, Devices, Control, and Applications: 10th International Conference, EuroHaptics 2016, London, UK, July 4-7, 2016, Proceedings, Part I*, pages 180–189. Springer International Publishing, Cham.

[Ho and Hirai, 2017] Ho, V. A. and Hirai, S. (2017). From localized shearing to localized slippage perception. In *2016 International Symposium on Experimental Robotics*, pages 443–453. Springer International Publishing, Cham.

[Hollins et al., 2000] Hollins, M., Bensmaïa, S., Karlof, K., and Young, F. (2000). Individual differences in perceptual space for tactile textures: Evidence from multidimensional scaling. *Perception & Psychophysics*, 62(8):1534–1544.

[Hollins et al., 1993] Hollins, M., Faldowski, R., Rao, S., and Young, F. (1993). Perceptual dimensions of tactile surface texture: A multidimensional scaling analysis. *Perception & Psychophysics*, 54(6):697–705.

[Hollins and Risner, 2000] Hollins, M. and Risner, S. R. (2000). Evidence for the duplex theory of tactile texture perception. *Perception & Psychophysics*, 62(4):695–705.

[Ilkhani et al., 2017] Ilkhani, G., Aziziaghdam, M., and Samur, E. (2017). Data-driven texture rendering on an electrostatic tactile display. *International Journal of HumanComputer Interaction*, 33(9):756–770.

[Jiao et al., 2018] Jiao, J., Zhang, Y., Wang, D., Visell, Y., Cao, D., Guo, X., and Sun, X. (2018). Data-driven rendering of fabric textures on electrostatic tactile displays. In *IEEE Haptics Symposium (HAPTICS)*, pages 169–174.

[Johnson, 2001] Johnson, K. O. (2001). The roles and functions of cutaneous mechanoreceptors. *Current Opinion in Neurobiology*, 11 4:455–461.

[Johnson et al., 2000] Johnson, K. O., Yoshioka, T., and Vega Bermudez, F. (2000). Tactile functions of mechanoreceptive afferents innervating the hand. *Journal of Clinical Neurophysiology*, 17(6):539–558.

[Jones and Tan, 2013] Jones, L. A. and Tan, H. Z. (2013). Application of psychophysical techniques to haptic research. *IEEE Transactions on Haptics*, 6(3):268–284.

[Kalantari et al., 2016] Kalantari, F., Grisoni, L., Giraud, F., and Rekik, Y. (2016). Finding the minimum perceivable size of a tactile element on an ultrasonic based haptic tablet. In *Proceedings of the ACM International Conference on Interactive Surfaces and Spaces*, ISS '16, pages 379–384, New York, NY, USA. ACM.

[Kalantari et al., 2018] Kalantari, F., Lank, E., Rekik, Y., Grisoni, L., and Giraud, F. (2018). Determining the haptic feedback position for optimizing the targeting performance on ultrasonic tactile displays. In *IEEE Haptics Symposium (HAPTICS)*, pages 204–209.

[Kim et al., 2015] Kim, J., Son, K. J., and Kim, K. (2015). An empirical study of rendering sinusoidal textures on a ultrasonic variable-friction haptic surface. In *12th International Conference on Ubiquitous Robots and Ambient Intelligence (URAI)*, pages 593–596.

[Kim et al., 2013] Kim, S.-C., Israr, A., and Poupyrev, I. (2013). Tactile rendering of 3D features on touch surfaces. In *Proceedings of the 26th Annual ACM Symposium on User Interface Software and Technology*, UIST '13, pages 531–538, New York, NY, USA. ACM.

[Klatzky and Lederman, 1999] Klatzky, R. L. and Lederman, S. J. (1999). Tactile roughness perception with a rigid link interposed between skin and surface. *Perception & psychophysics*, 61(4):591–607.

[Klatzky and Lederman, 2006] Klatzky, R. L. and Lederman, S. J. (2006). The perceived roughness of resistive virtual textures: I. Rendering by a force-feedback mouse. *ACM Trans. Appl. Percept.*, 3(1):1–14.

[Klatzky et al., 2003] Klatzky, R. L., Lederman, S. J., Hamilton, C., Grindley, M., and Swendsen, R. H. (2003). Feeling textures through a probe: Effects of probe and surface geometry and exploratory factors. *Perception & Psychophysics*, 65(4):613–631.

[Kocsis et al., 2013] Kocsis, M. B., Cholewiak, S. A., Traylor, R. M., Adelstein, B. D., Hirleman, E. D., and Tan, H. Z. (2013). Discrimination of real and virtual surfaces with sinusoidal and triangular gratings using the fingertip and stylus. *IEEE Transactions on Haptics*, 6(2):181–192.

[Kornbrot et al., 2007] Kornbrot, D., Penn, P., Petrie, H., Furner, S., and Hardwick, A. (2007). Roughness perception in haptic virtual reality for sighted and blind people. *Perception and Psychophysics*, 69(4):502–512.

[Lawrence et al., 2007] Lawrence, M. A., Kitada, R., Klatzky, R. L., and Lederman, S. J. (2007). Haptic roughness perception of linear gratings via bare finger or rigid probe. *Perception*, 36(4):547–557.

[Lederman, 1974] Lederman, S. J. (1974). Tactile roughness of grooved surfaces: The touching process and effects of macro- and microsurface structure. *Perception & Psychophysics*, 16(2):385–395.

[Lederman, 1983] Lederman, S. J. (1983). Tactual roughness perception: Spatial and temporal determinants. *Canadian Journal of Psychology*, 37(4):498–511.

[Lederman et al., 2006] Lederman, S. J., Klatzky, R. L., Tong, C., and Hamilton, C. (2006). The perceived roughness of resistive virtual textures: II. Effects of varying viscosity with a force-feedback device. *ACM Trans. Appl. Percept.*, 3(1):15–30.

[Lederman and Taylor, 1972] Lederman, S. J. and Taylor, M. M. (1972). Fingertip force, surface geometry, and the perception of roughness by active touch. *Perception & Psychophysics*, 12(5):401–408.

[Meftah et al., 2000] Meftah, E. M., Belingard, L., and Chapman, C. E. (2000). Relative effects of the spatial and temporal characteristics of scanned surfaces on human perception of tactile roughness using passive touch. *Experimental Brain Research*, 132(3):351–361.

[Messaoud et al., 2016a] Messaoud, W. B., Bueno, M.-A., and Lemaire-Semail, B. (2016a). Relation between human perceived friction and finger friction characteristics. *Tribology International*, 98:261 – 269.

[Messaoud et al., 2016b] Messaoud, W. B., Giraud, F., Lemaire-Semail, B., Amberg, M., and Bueno, M. A. (2016b). Amplitude control of an ultrasonic vibration for a tactile stimulator. *IEEE/ASME Transactions on Mechatronics*, 21(3):1692–1701.

[Meyer et al., 2015] Meyer, D. J., Peshkin, M. A., and Colgate, J. E. (2015). Modeling and synthesis of tactile texture with spatial spectrograms for display on variable friction surfaces. In *IEEE World Haptics Conference (WHC)*, pages 125–130.

[Meyer et al., 2014] Meyer, D. J., Wiertlewski, M., Peshkin, M. A., and Colgate, J. E. (2014). Dynamics of ultrasonic and electrostatic friction modulation for rendering texture on haptic surfaces. In *2014 IEEE Haptics Symposium (HAPTICS)*, pages 63–67.

[Monnoyer et al., 2016] Monnoyer, J., Diaz, E., Bourdin, C., and Wiertlewski, M. (2016). *Ultrasonic Friction Modulation While Pressing Induces a Tactile Feedback*, pages 171–179. Springer International Publishing, Cham.

[Monnoyer et al., 2017] Monnoyer, J., Diaz, E., Bourdin, C., and Wiertlewski, M. (2017). Optimal skin impedance promotes perception of ultrasonic switches. In *IEEE World Haptics Conference (WHC)*, pages 130–135.

[Morley et al., 1983] Morley, J. W., Goodwin, A. W., and Darian-Smith, I. (1983). Tactile discrimination of gratings. *Experimental Brain Research*, 49(2):291–299.

[Moscatelli et al., 2014] Moscatelli, A., Naceri, A., and Ernst, M. O. (2014). Path integration in tactile perception of shapes. *Behavioural Brain Research*, 274:355 – 364.

[Moy et al., 2000] Moy, G., Singh, U., Tan, E., and Fearing, R. S. (2000). Human psychophysics for teletaction system design. *Haptics-e Journal*, 1(3).

[Nefs et al., 2001] Nefs, H. T., Kappers, A. M. L., and Koenderink, J. J. (2001). Amplitude and spatial-period discrimination in sinusoidal gratings by dynamic touch. *Perception*, 30(10):1263–1274.

[Okamoto et al., 2013] Okamoto, S., Nagano, H., and Yamada, Y. (2013). Psychophysical dimensions of tactile perception of textures. *IEEE Transactions on Haptics*, 6(1):81–93.

[Osgouei et al., 2017] Osgouei, R. H., Kim, J. R., and Choi, S. (2017). Improving 3D shape recognition with electrostatic friction display. *IEEE Transactions on Haptics*, 10(4):533–544.

[Osgouei et al., 2018] Osgouei, R. H., Shin, S., Kim, J. R., and Choi, S. (2018). An inverse neural network model for data-driven texture rendering on electrovibration display. In *IEEE Haptics Symposium (HAPTICS)*, pages 270–277.

[Paré et al., 2002] Paré, M., Carnahan, H., and Smith, A. M. (2002). Magnitude estimation of tangential force applied to the fingerpad. *Experimental Brain Research*, 142(3):342–348.

[Pasumarty et al., 2011] Pasumarty, S. M., Johnson, S. A., Watson, S. A., and Adams, M. J. (2011). Friction of the human finger pad: Influence of moisture, occlusion and velocity. *Tribology Letters*, 44(2):117.

[Ramalho et al., 2013] Ramalho, A., Szekeres, P., and Fernandes, E. (2013). Friction and tactile perception of textile fabrics. *Tribology International*, 63:29 – 33.

[Rekik et al., 2017] Rekik, Y., Vezzoli, E., Grisoni, L., and Giraud, F. (2017). Localized haptic texture: A rendering technique based on taxels for high density tactile feedback. In *Proceedings of the 2017 CHI Conference on Human Factors in Computing Systems*, CHI '17, pages 5006–5015, New York, NY, USA. ACM.

[Saleem et al., 2017] Saleem, M. K., Yilmaz, C., and Basdogan, C. (2017). Tactile perception of change in friction on an ultrasonically actuated glass surface. In *2017 IEEE World Haptics Conference (WHC)*, pages 495–500.

[Samur et al., 2009] Samur, E., Colgate, J. E., and Peshkin, M. A. (2009). Psychophysical evaluation of a variable friction tactile interface. In *International Conference on Perception and Cognition in Electronics Media, San Jose, California*.

[Sathian et al., 1989] Sathian, K., Goodwin, A. W., John, K. T., and Darian-Smith, I. (1989). Perceived roughness of a grating: correlation with responses of mechanoreceptive afferents innervating the monkey's fingerpad. *Journal of Neuroscience*, 9(4):1273–1279.

[Sednaoui et al., 2015] Sednaoui, T., Vezzoli, E., Dzidek, B., Lemaire-Semail, B., Chappaz, C., and Adams, M. (2015). Experimental evaluation of friction reduction in ultrasonic devices. In *2015 IEEE World Haptics Conference (WHC)*, pages 37–42.

[Sednaoui et al., 2017] Sednaoui, T., Vezzoli, E., Dzidek, B., Lemaire-Semail, B., Chappaz, C., and Adams, M. (2017). Friction reduction through ultrasonic vibration part 2: Experimental evaluation of intermittent contact and squeeze film levitation. *IEEE Transactions on Haptics*, 10(2):208–216.

[Shull et al., 2010] Shull, P., Bark, K., and Cutkosky, M. (2010). Skin nonlinearities and their effect on user perception for rotational skin stretch. In *IEEE Haptics Symposium*, pages 77–82.

[Shultz et al., 2015] Shultz, C. D., Peshkin, M. A., and Colgate, J. E. (2015). Surface haptics via electroadhesion: Expanding electrovibration with Johnsen and Rahbek. In *IEEE World Haptics Conference (WHC)*, pages 57–62.

[Smith et al., 2010] Smith, A. M., Basile, G., Theriault-Groom, J., Fortier-Poisson, P., Campion, G., and Hayward, V. (2010). Roughness of simulated surfaces examined with a haptic tool: effects of spatial period, friction, and resistance amplitude. *Experimental Brain Research*, 202:33–43.

[Smith et al., 2002] Smith, A. M., Chapman, C. E., Deslandes, M., Langlais, J.-S., and Thibodeau, M.-P. (2002). Role of friction and tangential force variation in the subjective scaling of tactile roughness. *Experimental Brain Research*, 144(2):211–223.

[Smith and Scott, 1996] Smith, A. M. and Scott, S. H. (1996). Subjective scaling of smooth surface friction. *Journal of Neurophysiology*, 75(5):1957–1962.

[Srinivasan et al., 1990] Srinivasan, M. A., Whitehouse, J. M., and LaMotte, R. H. (1990). Tactile detection of slip: surface microgeometry and peripheral neural codes. *Journal of Neurophysiology*, 63(6):1323–1332.

[Sutu et al., 2013] Sutu, A., Meftah, E.-M., and Chapman, C. E. (2013). Physical determinants of the shape of the psychophysical curve relating tactile roughness to raised-dot spacing: implications for neuronal coding of roughness. *Journal of Neurophysiology*, 109(5):1403–1415.

[Tanaka et al., 2014] Tanaka, Y., Bergmann Tiest, W. M., Kappers, A. M. L., and Sano, A. (2014). Contact force and scanning velocity during active roughness perception. *PLOS ONE*, 9(3):1–11.

[Tashiro et al., 2009] Tashiro, K., Shiokawa, Y., Aono, T., and Maeno, T. (2009). Realization of button click feeling by use of ultrasonic vibration and force feedback. In *World Haptics 2009 - Third Joint EuroHaptics conference and Symposium on Haptic Interfaces for Virtual Environment and Teleoperator Systems*, pages 1–6.

[Taylor and Lederman, 1975] Taylor, M. M. and Lederman, S. J. (1975). Tactile roughness of grooved surfaces: A model and the effect of friction. *Perception & Psychophysics*, 17(1):23–36.

[Tymms et al., 2018] Tymms, C., Zorin, D., and Gardner, E. P. (2018). Tactile perception of the roughness of 3D-printed textures. *Journal of Neurophysiology*, 119(3):862–876.

[Unger et al., 2011] Unger, B., Hollis, R., and Klatzky, R. (2011). Roughness perception in virtual textures. *IEEE Transactions on Haptics*, 4(2):122–133.

[Vardar et al., 2017a] Vardar, Y., Guclu, B., and Basdogan, C. (2017a). Effect of waveform on tactile perception by electrovibration displayed on touch screens. *IEEE Transactions on Haptics*, 10(4):488–499.

[Vardar et al., 2017b] Vardar, Y., Isleyen, A., Saleem, M. K., and Basdogan, C. (2017b). Roughness perception of virtual textures displayed by electrovibration on touch screens. In *IEEE World Haptics Conference (WHC)*, pages 263–268.

[Vezzoli et al., 2016] Vezzoli, E., Sednaoui, T., Amberg, M., Giraud, F., and Lemaire-Semail, B. (2016). Texture rendering strategies with a high fidelity-capacitive visual-haptic friction control device. In Bello, F., Kajimoto, H., and Visell, Y., editors, *International Conference on Human Haptic Sensing and Touch Enabled Computer Applications*, pages 251–260.

[Vezzoli et al., 2017] Vezzoli, E., Vidrih, Z., Giamundo, V., Lemaire-Semail, B., Giraud, F., Rodic, T., Peric, D., and Adams, M. (2017). Friction reduction through ultrasonic vibration part 1: Modelling intermittent contact. *IEEE Transactions on Haptics*, 10(2):196–207.

[Wang and Hayward, 2007] Wang, Q. and Hayward, V. (2007). In vivo biomechanics of the fingerpad skin under local tangential traction. *Journal of Biomechanics*, 40(4):851 – 860.

[Ware et al., 2014] Ware, J., Cha, E., Peshkin, M. A., Colgate, J. E., and Klatzky, R. L. (2014). Search efficiency for tactile features rendered by surface haptic displays. *IEEE Transactions on Haptics*, 7(4):545–550.

[Watanabe and Fukui, 1995] Watanabe, T. and Fukui, S. (1995). A method for controlling tactile sensation of surface roughness using ultrasonic vibration. In *Proceedings of IEEE International Conference on Robotics and Automation*, volume 1, pages 1134–1139 vol.1.

[Weber et al., 2013] Weber, A. I., Saal, H. P., Lieber, J. D., Cheng, J.-W., Manfredi, L. R., Dammann, J. F., and Bensmaia, S. J. (2013). Spatial and temporal codes mediate the tactile perception of natural textures. *Proceedings of the National Academy of Sciences*, 110(42):17107–17112.

[Wiertlewski et al., 2016] Wiertlewski, M., Fenton Friesen, R., and Colgate, J. E. (2016). Partial squeeze film levitation modulates fingertip friction. *Proceedings of the National Academy of Sciences*, 113(33):9210–9215.

[Won et al., 2017] Won, S. Y., Kim, H. K., and Kim, K. S. (2017). Two-point discrimination values vary depending on test site, sex and test modality in the orofacial region: a preliminary study. *J Appl Oral Sci.*, 25(4):427–35.

[Yoshioka et al., 2001] Yoshioka, T., Gibb, B., Dorsch, A. K., Hsiao, S. S., and Johnson, K. O. (2001). Neural coding mechanisms underlying perceived roughness of finely textured surfaces. *Journal of Neuroscience*, 21(17):6905–6916.

[Zhang and Harrison, 2015] Zhang, Y. and Harrison, C. (2015). Quantifying the targeting performance benefit of electrostatic haptic feedback on touchscreens. In *Proceedings of the International Conference on Interactive Tabletops & Surfaces*, ITS '15, pages 43–46, New York, NY, USA. ACM.

[Zwislocki and Relkin, 2001] Zwislocki, J. J. and Relkin, E. M. (2001). On a psychophysical transformed-rule up and down method converging on a 75% level of correct responses. *Proceedings of the National Academy of Sciences*, 98(8):4811–4814.